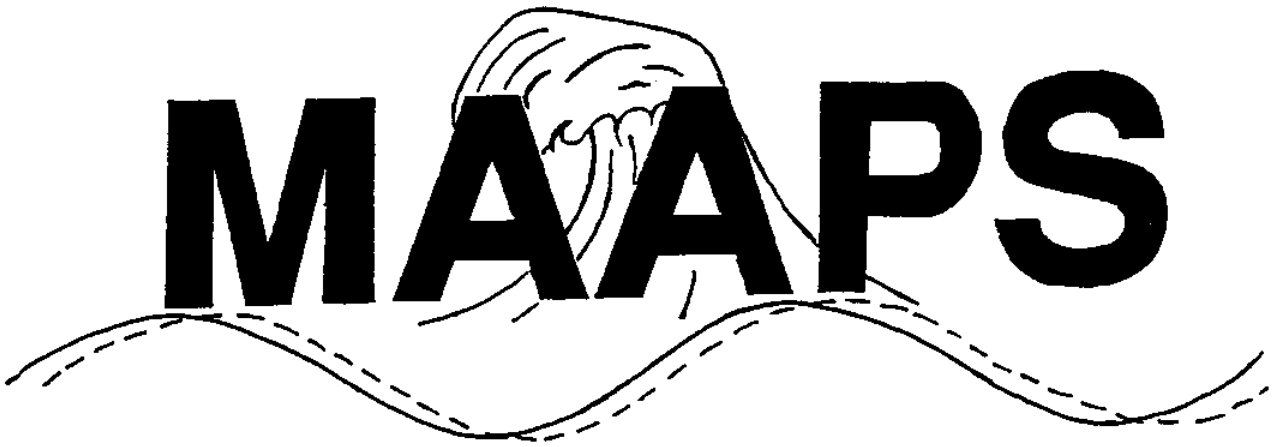

Measurement of
Aquatic
Acoustic
Propagation
Speed

Direct Measurement Underwater Acoustic Velocimeter

UNH TECH 697 (1990)

Project Team:
Ben Wallace
Jon Wilson
Alan Young
Advisor:
Prof. Ken Baldwin

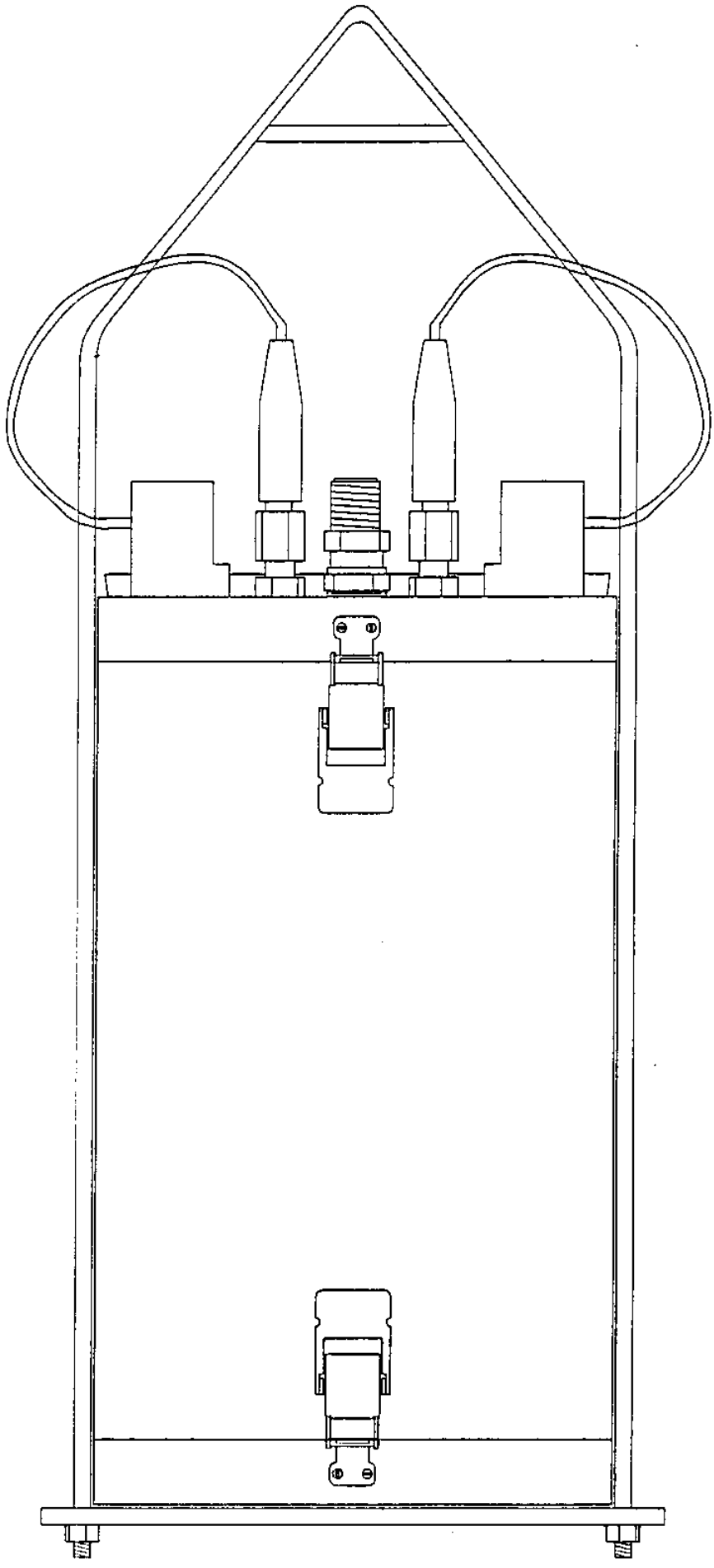

ACKNOWLEDGEMENTS AND THANKS

The MAAPS project team would like to extend a special thanks to Bob Doucette and Bob Blake at the UNH machine shop for their cooperation and invaluable experience in making the project a reality. Special thanks also goes to Dick Jennings for the use of the UNH Junior lab, John Woods of OPAL for all his help, and Jim Glynn for his help on the original design concept. We would also like to thank Carol in the MSEL lab for her help in handling the bureaucratic hassles involved with the project. Also thanks to D.G. Obrien and Sylvester Sheet Metal for their generosity and advice.

TABLE OF CONTENTS

1 - ABSTRACT

The MAAPS project is a complete system for the measurement and logging of temperature, pressure and acoustic velocities from surface level to a water depth of 2500 ft. Velocity measurements are made of a sound signal transmitted between two piezoelectric transducers mounted on the surface of the pressure vessel. The velocity measurement is achieved by comparing the phase shift of the sound wave that passes through the water medium to the undisturbed input signal. The velocity measurements are triggered at regular intervals by an on board computer. The water temperature measurements are be made through a thermistor and the depth is determined from a pressure transducer. All data is logged in a single board computer to be offloaded through an RS232 interface after the instrument is brought back to the surface. The unit is completely self contained in an aluminum housing and requires no operator interface once lowered into the water.

2 - INTRODUCTION

The MAAPS project (Measurement of Aquatic Acoustic Propagation Speed) is directed at developing a device for directly and accurately measuring sound velocity underwater as a function of temperature and depth. The resultant sound velocity profile (see fig. 1) is used in acoustic ray tracing.

Sound propagation underwater is directly dependent on the speed of sound at different depths. Varying sound velocity layers cause sound waves to refract as they pass from one layer to the next. The resulting path of the sound wave is shown in a ray tracing profile (see fig. 2). Understanding the behavior of sound underwater and being able to produce accurate ray tracing profiles is essential to many practical uses of sound for underwater communication or research. Since there already exists a method of ray tracing from the sound velocity profile it is the interest of this project to develop a more direct and easy to use device for measuring sound velocity.

Previous work in measuring underwater sound velocity was done in conjunction with measuring temperature, depth, and conductivity. The data were then reduced to establish empirical relationships for sound velocity as a function of conductivity, temperature, and depth. The emphasis was then shifted to make more accurate and reliable measurements of conductivity, temperature, and depth (CTD). The empirical relationships were used almost exclusively for sound velocity profile generation.

The CTD instrument has since evolved into a very reliable

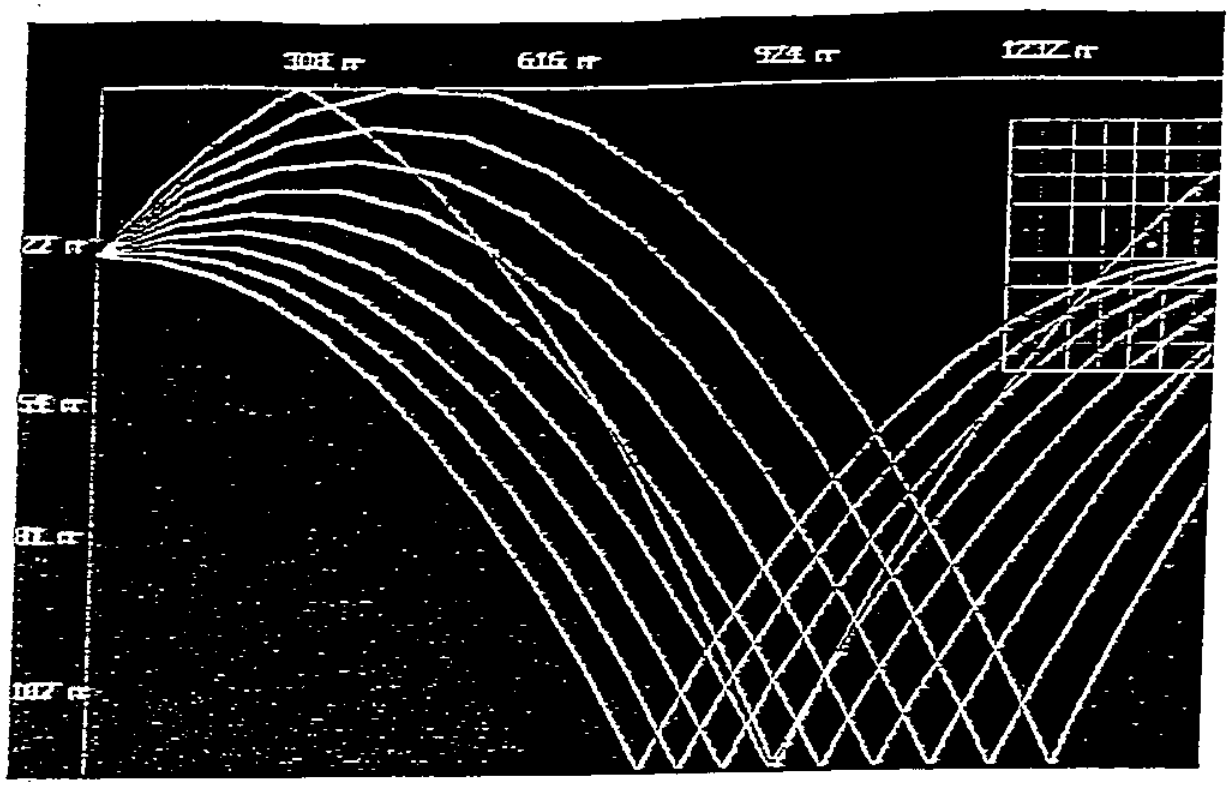

Ray Tracing Profile (from ref. 3)

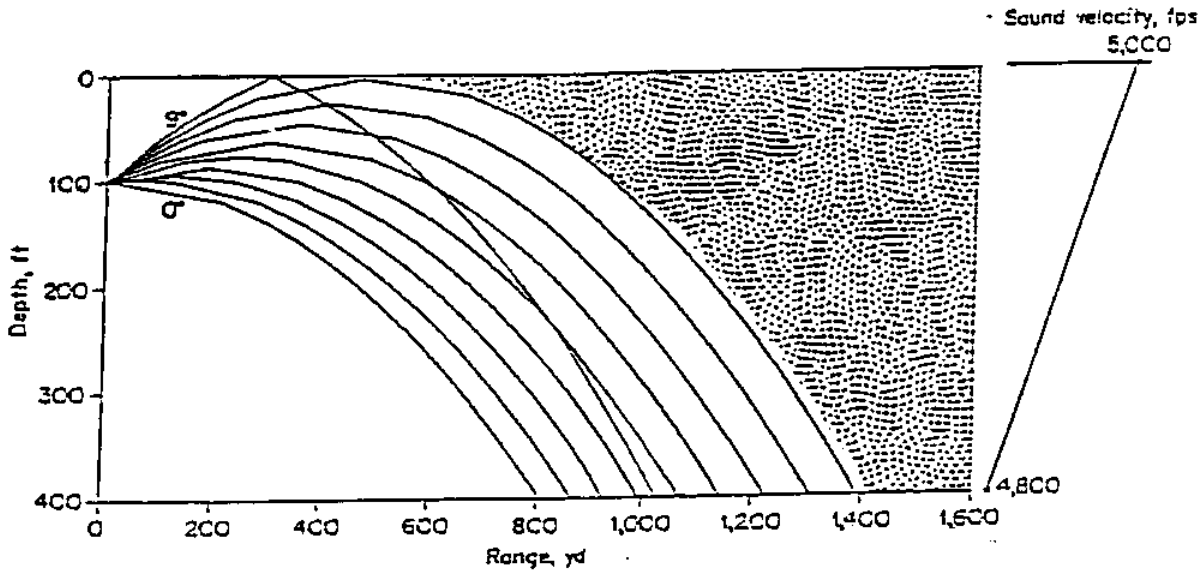

FIG. 2

Ray Tracing Profile (from ref. 1)

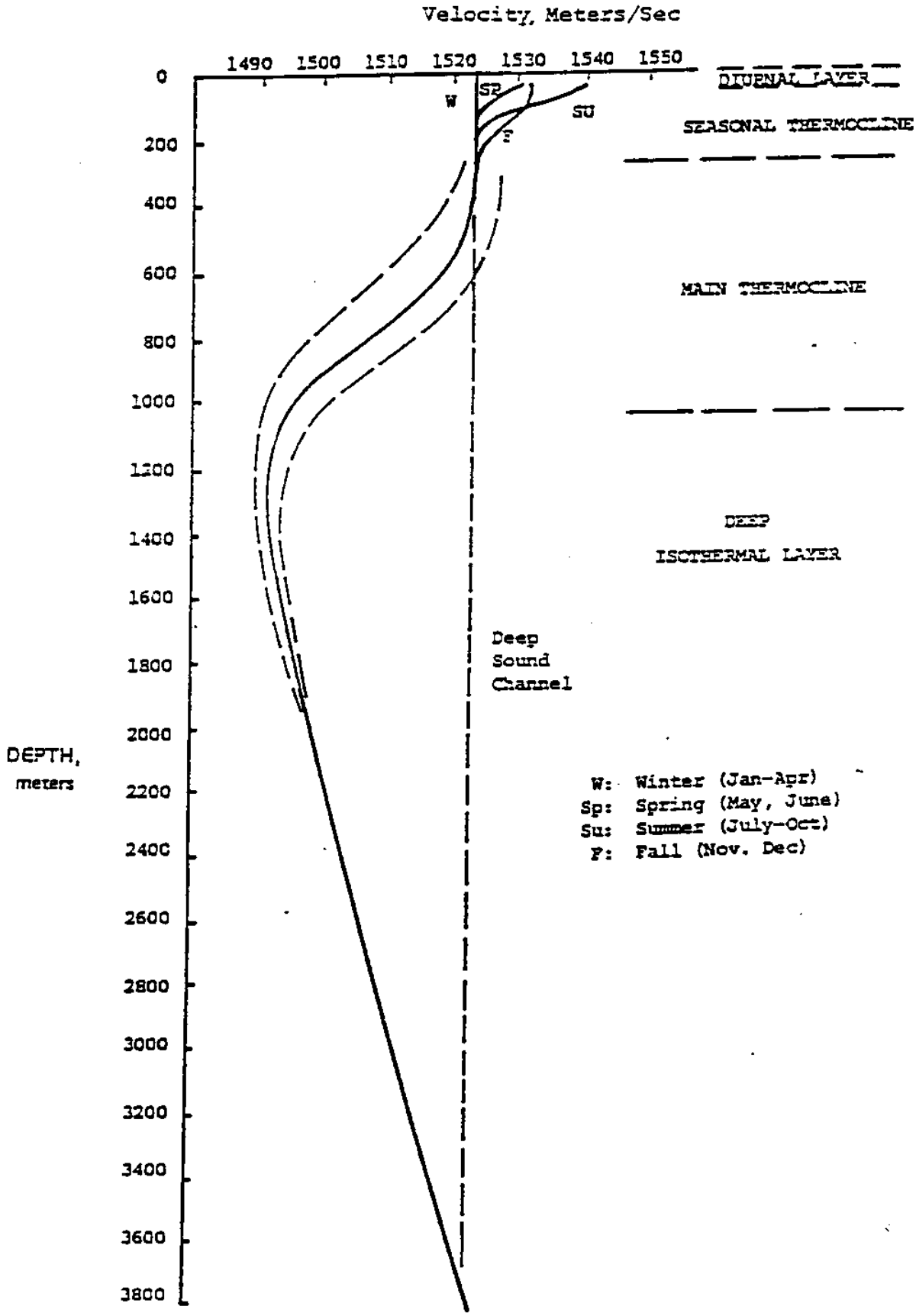

Deep Ocean Velocity Profile Based on Nansen casts taken every two weeks over a 9 year period at a location 15 miles SE of Bermuda.

FIG. 1

Velocity Profile (from ref. 2)

device while the direct measuring sound velocimeter has not received as much attention. There is evidence, however, that empirical relationships for sound velocity may not be sufficiently accurate to form reliable velocity profiles for acoustic ray tracing. Several common formulas for deriving sound velocity from temperature, salinity, and pressure disagree by 3 meters/sec. at zero depth and increases at greater depths. "Although apparently small, the difference sometimes results in large changes in ray diagrams, range computations, and travel times ..." (p.96, Ref.1). For this reason the development of a device for directly measuring sound velocity underwater is important to providing convincing velocity profiles for acoustic ray tracing.

3 - DESIGN CONSIDERATIONS

The primary mechanical design consideration for this project was to provide a waterproof housing for the instruments and electronics capable of withstanding the pressure at a depth of 2500 feet in sea water. A means of supporting the structure during operation was also to be designed.

The electronic hardware was designed to process incoming transducer data and store the data in a computer for later retrieval and processing. The computer's only task is that of data acquisition. It was decided that phase detection methods would be used to measure velocity. The phase difference between the transmitted and received signals are measured and the associated velocity calculated during post processing of the retrieved data.

The velocity differential from surface level to a depth of 2500 feet is approximately 50 meters per second. Within the scope of this project, it was decided that a resolution of one meter per second was an attainable goal.

Offloading data from the instrument was to be done on site. A means to do this without opening the instrument was therefore necessary to avoid the dangers of repeatedly breaking the instrument's seal under possibly adverse conditions.

4 - THEORY OF OPERATION

Phase detection measurement is based on the principal that the velocity of propagation is equal to the wavelength multiplied by the frequency of the signal. By maintaining a constant frequency, the wavelength becomes directly proportional to the velocity. A wave propagating through a medium such as water experiences a phase shift proportional to the change in its wavelength. The magnitude of this phase shift can be determined by comparing the shifted wave to the original unshifted waveform. The system block diagram of the MAAPS velocimeter is shown in figure 3. Velocity calculations are in appendix B.

5 - MECHANICAL DESIGN

The mechanical structure for the project (see fig. 4) is designed to provide a safe housing for the projects various instrumentation and electrical components while maintaining ease of operation during testing. The major design considerations include

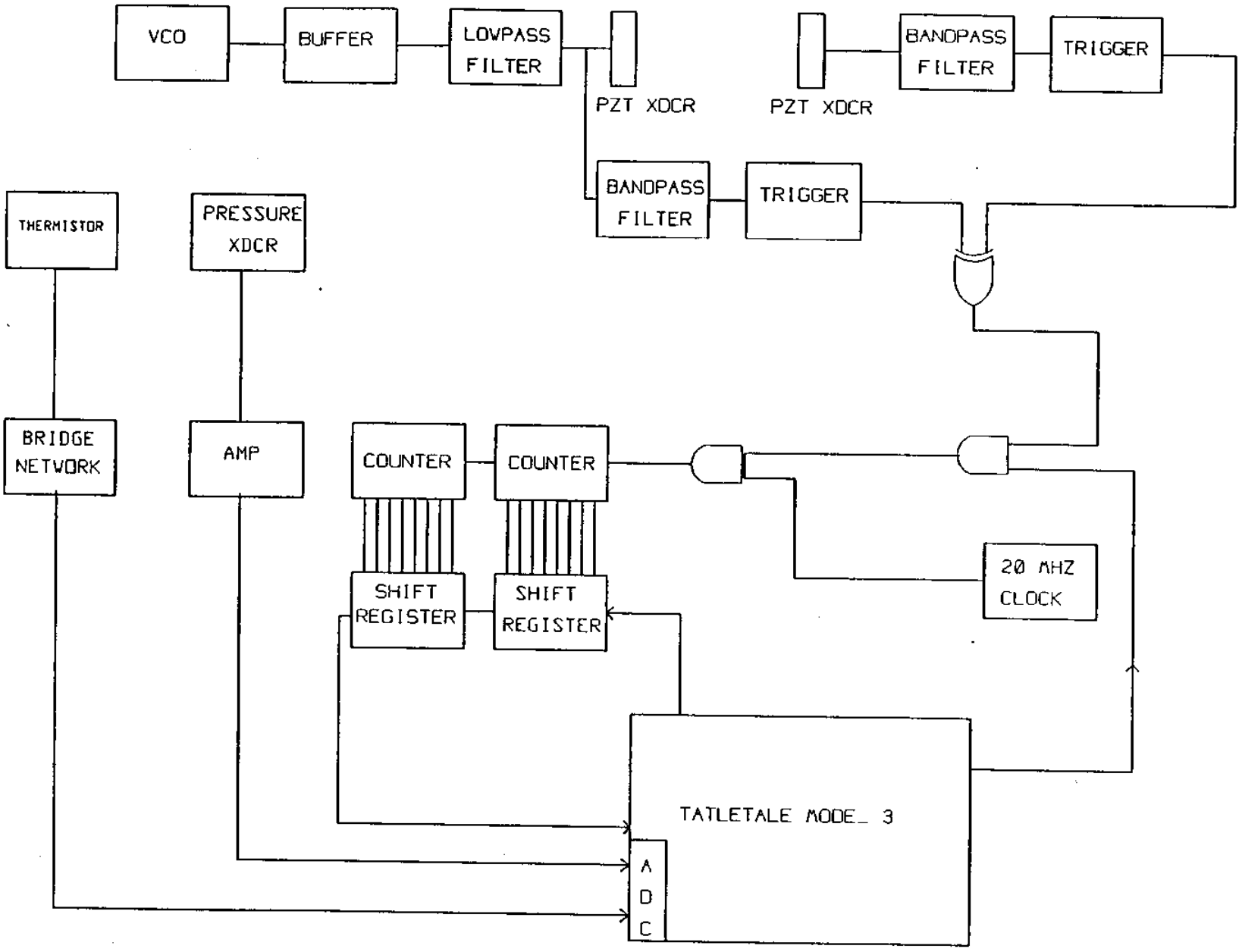

FIGURE 3 SYSTEM BLOCK DIAGRAM

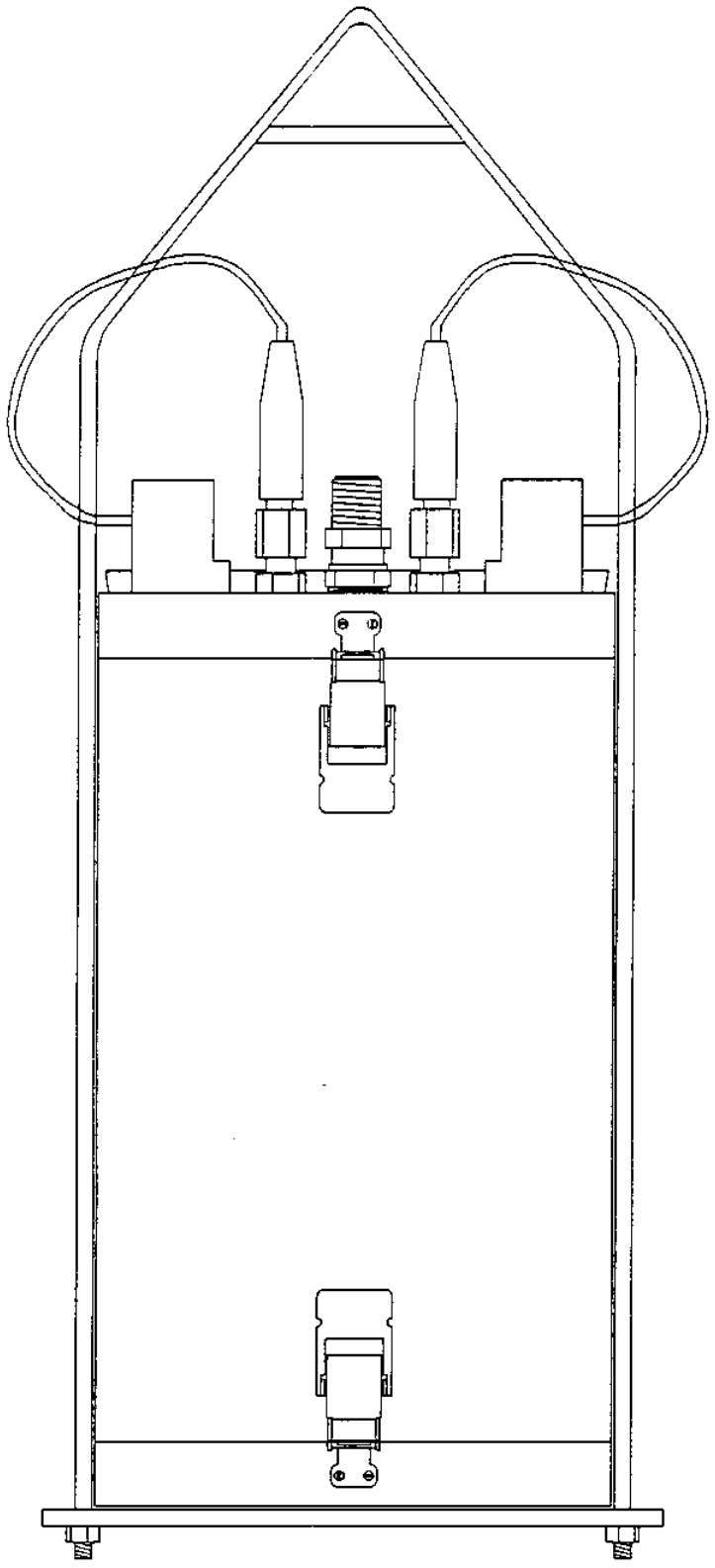

MAAPS PROJECT		
MAAPS TEAM : J. WILSON B. WALLACE A. YOUNG	ALL DIMENSIONS IN INCHES	COMPLETE INSTRUMENT
	SCALE -	DRAWING NAME OVERALL.DWG DATE: 2/15/90

FIGURE 4

a watertight and corrosion resistant housing unit strong enough to withstand pressures at 2500 ft and waterproof connections for all of the instrumentation. A supporting protective cage for the unit which protects the instrumentation and allows the unit to be lowered into the ocean easily was also designed.

5.1 - ALTERNATIVES

Research was done to study previous work in similar mechanical applications. Determination of materials, instrumentation and overall structure design were of concern. A CTD instrument which operated under similar conditions was found at the UNH Ocean Process Analysis Lab (OPAL). Based on that design and the particular needs of this project a conceptual mechanical design was formed (see fig. 5).

5.2 - PRESSURE VESSEL

A pressure vessel was required as the housing for the project (see fig. 6). Design criteria included strength of the cylinder and resistance to the ocean environment. Calculation of the operating pressure at 2500 ft. was made and found to be 1100 psi (see appendix A.1). Due to this high operating stress and the corrosive nature of salt water the Aluminum alloy 6061 T6 was chosen. The material properties of the alloy are shown in appendix A.2. To determine the mode of failure for the pressure vessel, collapse pressure (pressure to instability or buckling) was found to be 17132.35 psi and the yield pressure (pressure to induce

CONCEPTUAL DESIGN

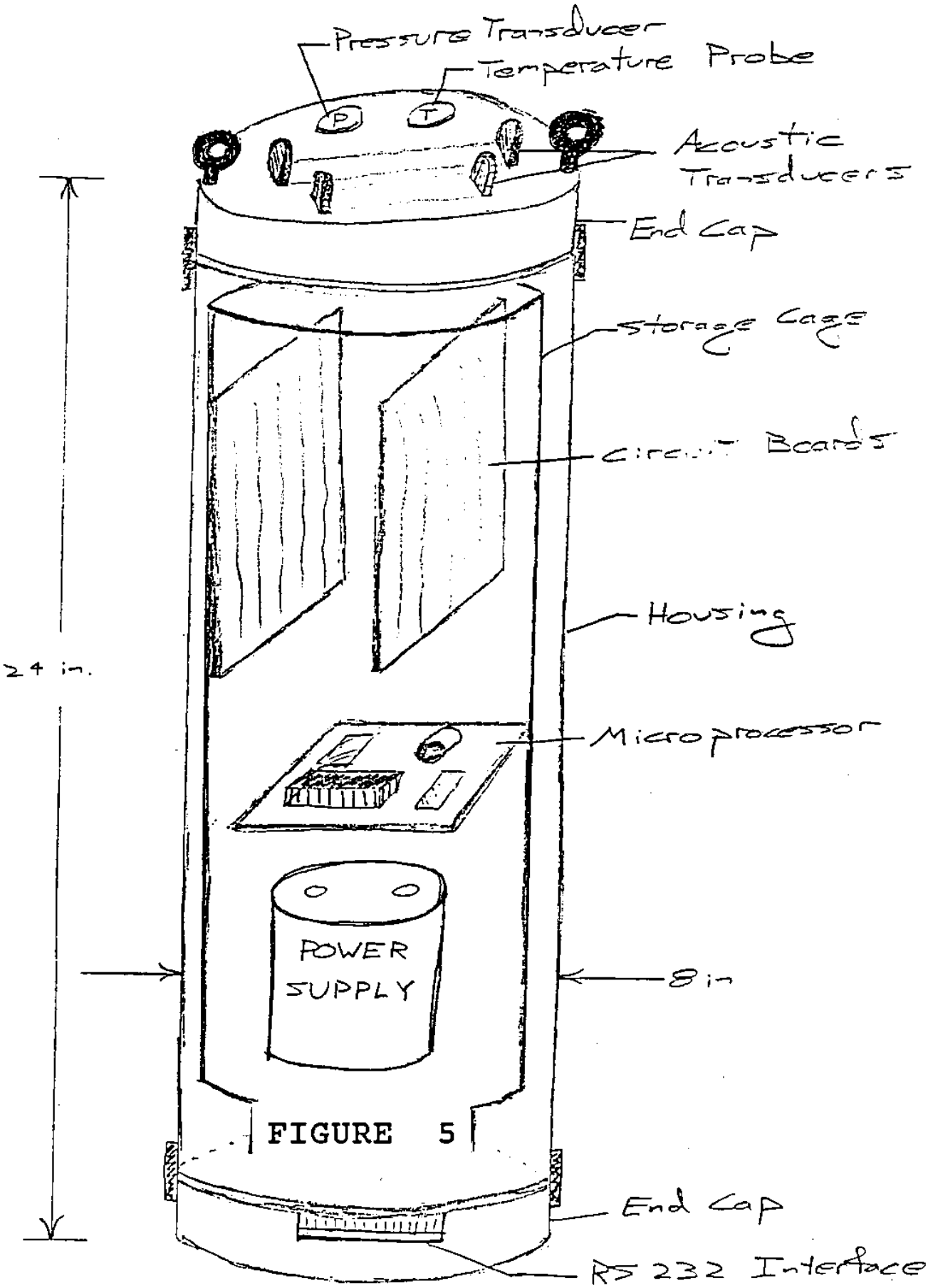

FIGURE 5

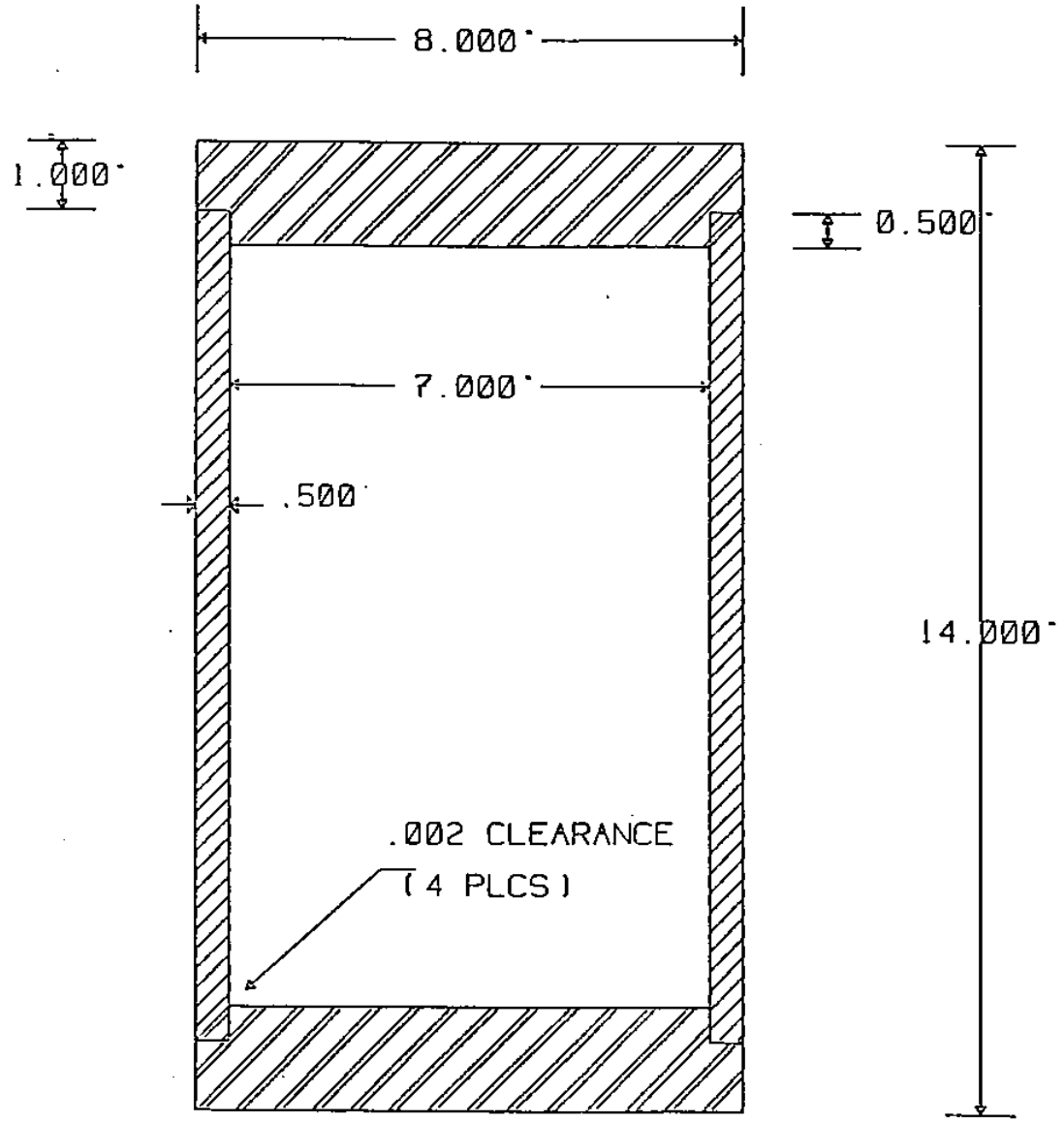

STANDARD TOLERANCE (.015 IN)

1" - 3"

1 SQUARE - .6"

MAAPS PROJECT		
MAAPS TEAM : J. WILSON B. WALLACE A. YOUNG	ALL DIMENSIONS IN INCHES	PRESSURE HOUSING LONGITUDINAL CROSS SECTION
	SCALE -	DRAWING NAME: HOUSING.DWG DATE: 2/15/90

FIGURE 6

yielding) was found to be 4375 psi (see Appendix A.3). Since yield pressure is well below collapse pressure it was assumed that failure would occur by yielding. The pressure analysis for yielding of the vessel was then calculated and found to provide a factor of safety of 3.73 for a cylinder with wall thickness of .5 in (see appendix A.4 and A.5).

While 6061 T6 aluminum is corrosion resistant it will pit with time in salt water. To solve this problem all aluminum parts were hard black anodized which not only protects the aluminum from corrosion but also resists scratches which can expose unprotected metal.

5.2.1 - END CAPS

End caps for the pressure vessel were designed to seal the cylinder and to provide a base for the instrumentation (see figures 7 & 8). Their design was based on the end caps of an existing CTD instrument in the UNH OPAL lab. Actual calculations to take into account the various holes drilled in the end caps were not feasible. The similarity to the OPAL CTD and its success in actual operation justified the design decision. To provide a watertight seal between the endcaps and pressure cylinder, two O-rings sit between each endcap and the cylinder (see fig 9). Selection of the O-rings were made using the Parker O-ring catalog (see appendix A.6).

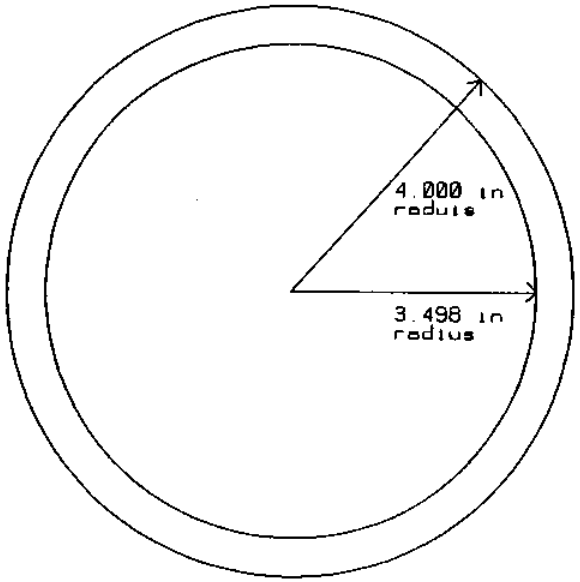

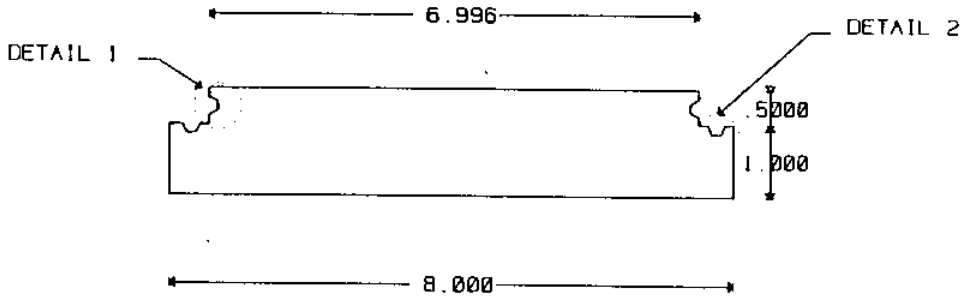

MAAPS PROJECT		
MAAPS TEAM : J. WILSON B. WALLACE A. YOUNG	ALL DIMENSIONS IN INCHES	PRESSURE HOUSING ENDCAP DESIGN
	SCALE -	DRAWING NAME: ENDCAP.DWG DATE: 2/15/90

FIGURE 7

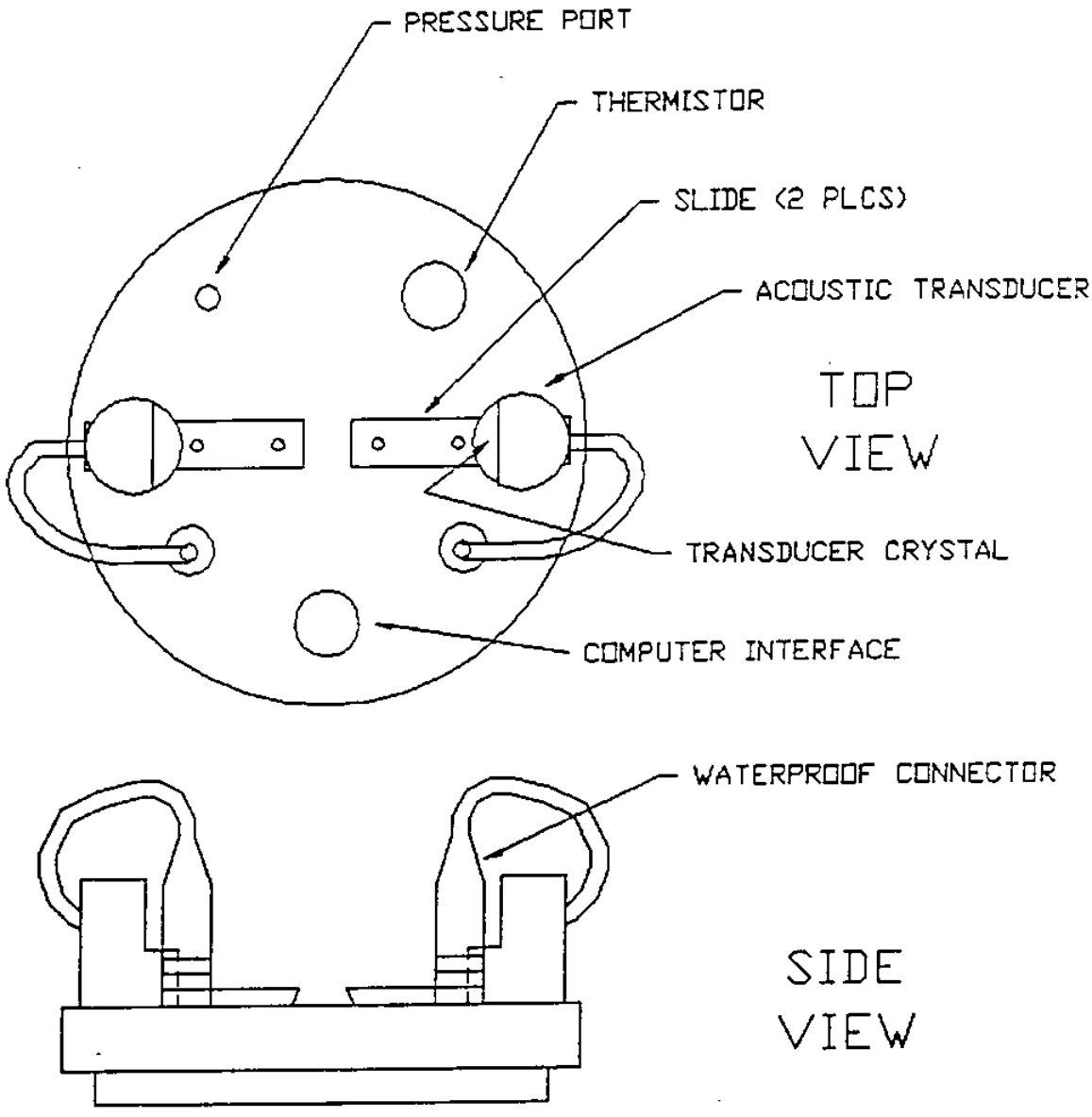

FIGURE 8

ENDCAP AND ACOUSTIC TRANSDUCER ASSEMBLY.

DETAIL 1
(2 PLCS)

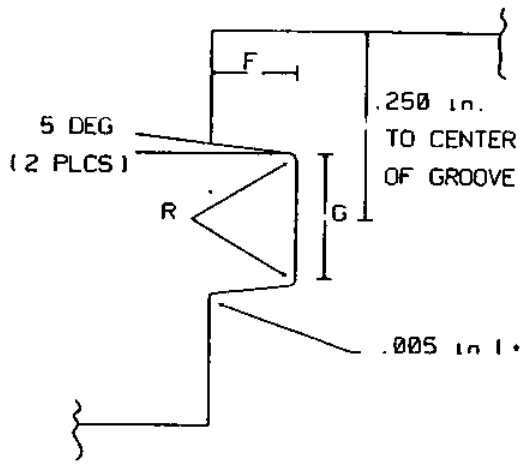

F=.110 in
G=.190 in
R=.018 in (+/- .005 in)

STANDARD TOLERANCE (+/- .015 in)

DETAIL 2
(2 PLCS)

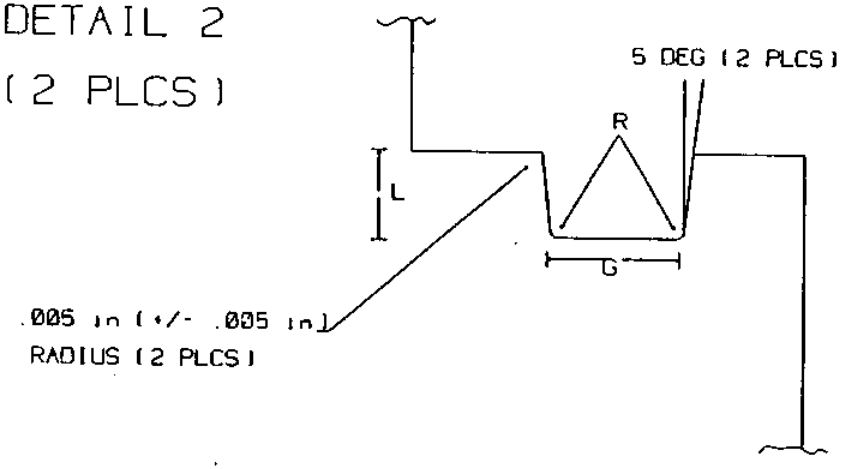

L=.104 in
G= .182 in
R= 018 in

MAAPS PROJECT		
MAAPS TEAM : J. WILSON B. WALLACE A. YOUNG	ALL DIMENSIONS IN INCHES	ENDCAP DETAILS : O RING GROOVES
	SCALE -	DRAWING NAME:DETAIL.DWG DATE: 2/15/90

FIGURE 9

5.3 - PROTECTIVE CARRYING CAGE

To lower the instrument into the water and to protect the external sensors, a protective carrying cage was designed (see figure 10). The carrying cage is constructed of stainless steel to resist corrosion. The cage is padded wherever the stainless steel comes in contact with the housing to avoid scratching the anodizing.

5.4 - PIEZOELECTRIC TRANSDUCER MOUNTINGS

Mountings were designed to hold the piezoelectric ceramic transducers used in the transmission of the acoustic signal (see figure 8). It was determined that the mass of the mounting directly behind the transducer must be three times the mass of the water column within one wavelength of the transmitted signal (see appendix B.1). This was to assure that a sufficient percent of the signal would propagate out the front of the transducer. The transducers were secured to the mountings using conductive epoxy. The transducer cavity was sealed using a non-conductive potting compound. To connect the transducers to the instruments internal circuitry, waterproof bulkhead connectors and cables were used. The mountings were secured on slides so the distance between them could be varied. During testing, it was found that the transducers were mechanically coupled through the endcap and the teflon slide. To remedy the situation the slide was cut into two sections and mounted on a rubber strip to insulate it from the endcap.

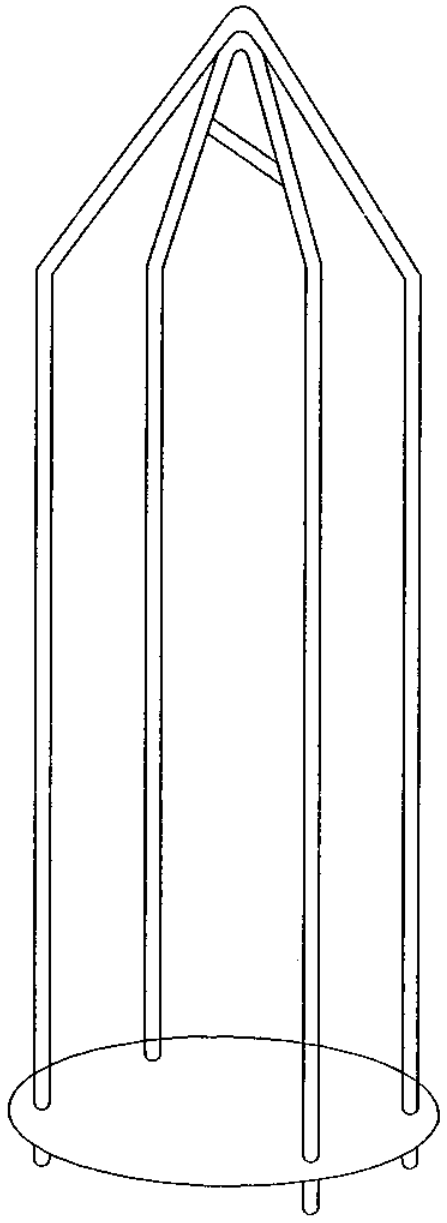

MAAPS PROJECT		
MAAPS TEAM : J. WILSON B. WALLACE A. YOUNG	ALL DIMENSIONS IN INCHES	PROTECTIVE CAGE
	SCALE -	DRAVING NAME:CRYCAGE.DVG DATE: 4-30-90

FIGURE 10

5.5 - CARD CAGE

The card cage provides a secure mounting for the circuitry, computer and power supply inside the cylinder (see figure 11). It is setup to allow for easy connections between the external sensors and the internal electrical components.

6 - ELECTRONIC DESIGN

6.1 - THERMISTOR ASSEMBLY

Temperature was measured using an external thermistor and a Wheatstone bridge network. Unsuccessful attempts to purchase a thermistor assembly designed for high pressure marine applications led to the decision to build an assembly using a single glass bead thermistor and a two terminal bulkhead connector. The thermistor bead was attached to the connector, surrounded by PVC tubing, and filled with a non conductive waterproof epoxy to protect the bead from breakage (see figure 12).

To obtain the resistance characteristics of the thermistor, it was immersed in water and tested at specific temperatures. The resistance was found to be a logarithmic function of temperature (see appendix C.1). For this reason the thermistor was placed in a Wheatstone bridge to linearize the output voltage (see appendix C.2). The thermistor was placed in one of the top legs of the bridge. Opposite the thermistor was placed a resistor equal to the value of the thermistor at zero degrees Celsius, the lowest temperature being measured. The resistors in the two lower legs of the bridge were chosen to be equal to the value of the

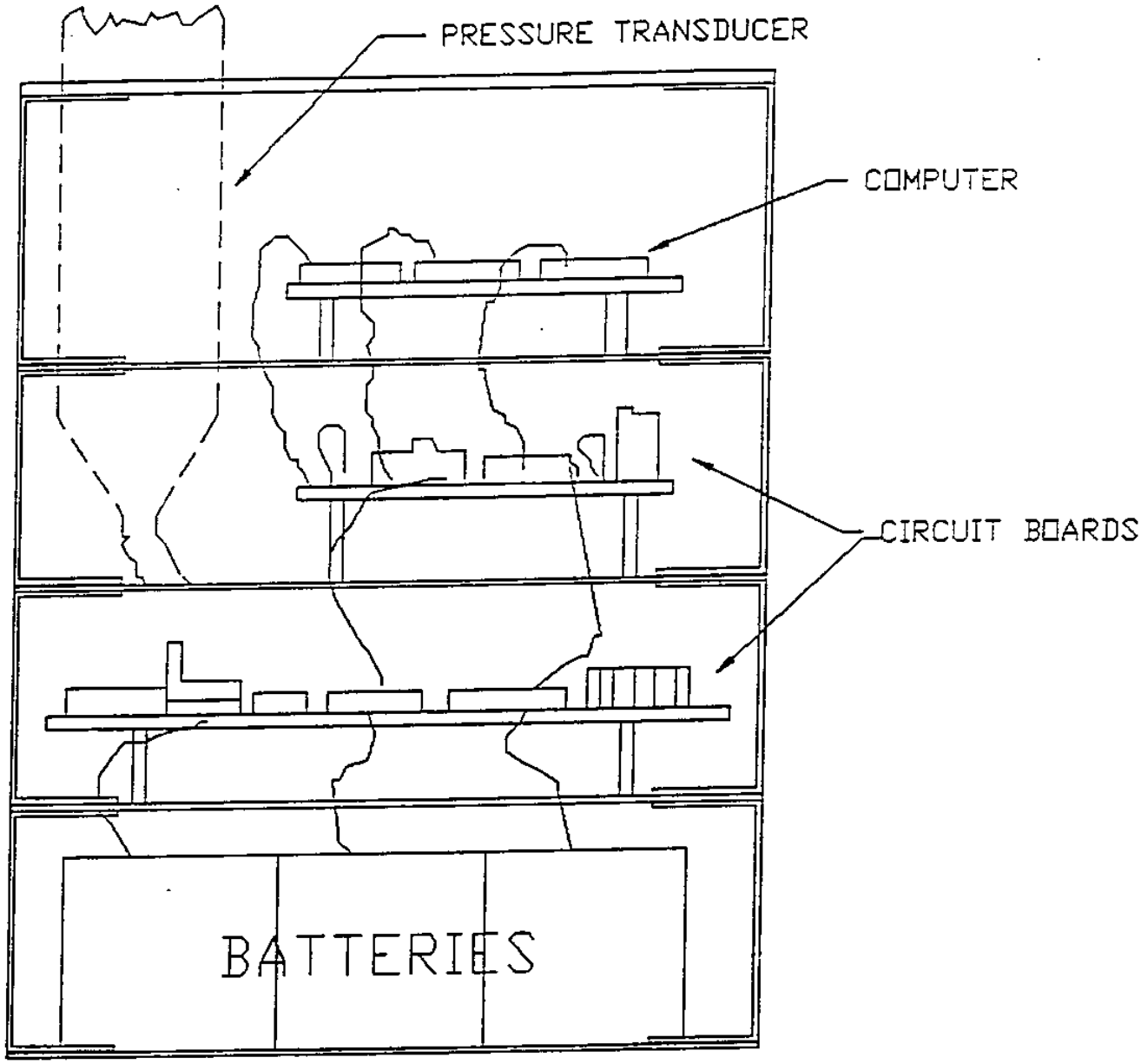

FIGURE 11

CARD CAGE

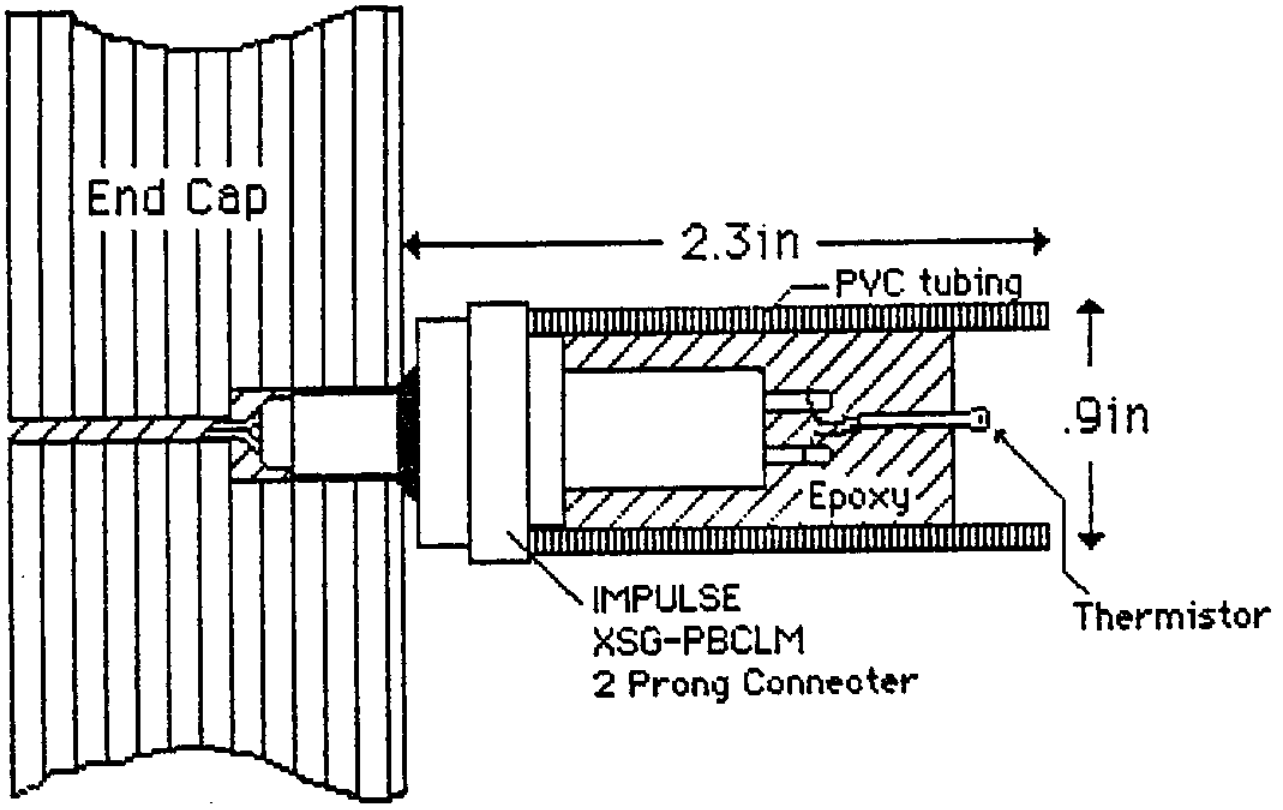

Thermistor Assembly

FIGURE 12

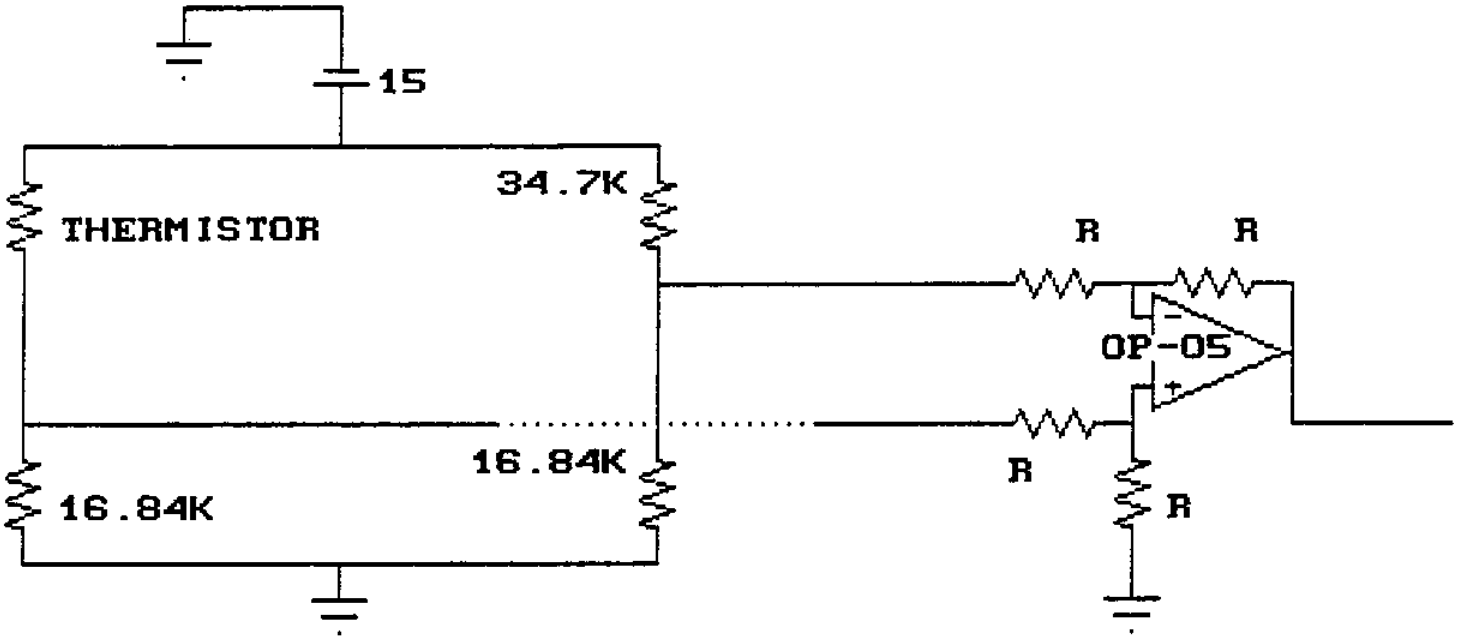

THERMISTOR CIRCUIT

FIGURE 13

6.3 - VELOCITY MEASUREMENT CIRCUITRY

6.3.1 - VOLTAGE CONTROLLED OSCILLATOR

The signal used to create the reference signal and to drive the source transducer was created using a single chip ICL8038 waveform generator. The generator provides for square, triangle and sine wave outputs. Set up in the configuration shown in figure 14, the generator will create these waves with a 50% duty cycle at a frequency of

$$f_o = 0.3 / RC. \qquad (2)$$

For calibration purposes, the circuit was wired to allow access to the triangular wave. The sharp, easily distinguishable transitions were used to establish a fifty percent duty cycle. This symmetry was adjusted using the trim pot R_{SYM}. The trim pot R_{THD} was used to adjust the total harmonic distortion of the signal.

The output of the generator was buffered before being filtered. A 180KHz low pass filter was used prior to the transmission of the signal for the purpose of removing the higher harmonics and creating a true sine wave (see figures 15 & 16).

6.3.2 - FILTERS

The first filter removes distortion introduced to the signal by the ocean environment. The filter is configured as a second order infinite gain, multiple feedback (IGMF) band pass filter. The circuit diagram and frequency response for this configuration are shown in figures 17 & 18.

The second filter was designed to be identical to the first

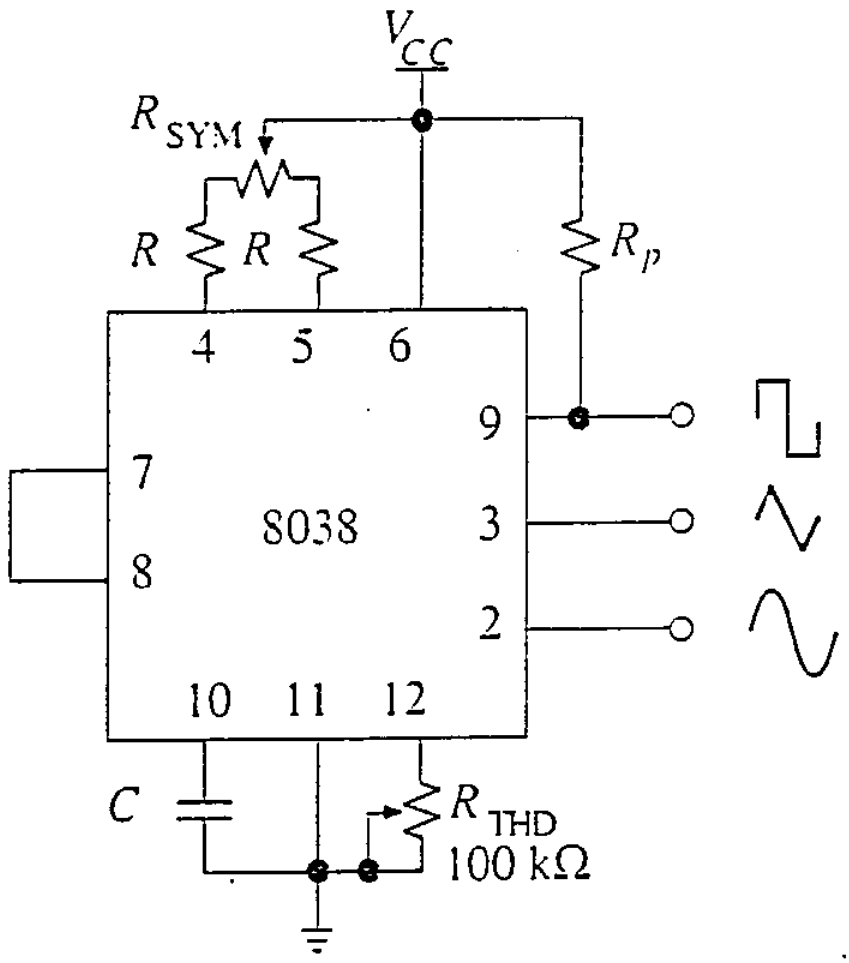

VCO CIRCUITRY

FIGURE 14

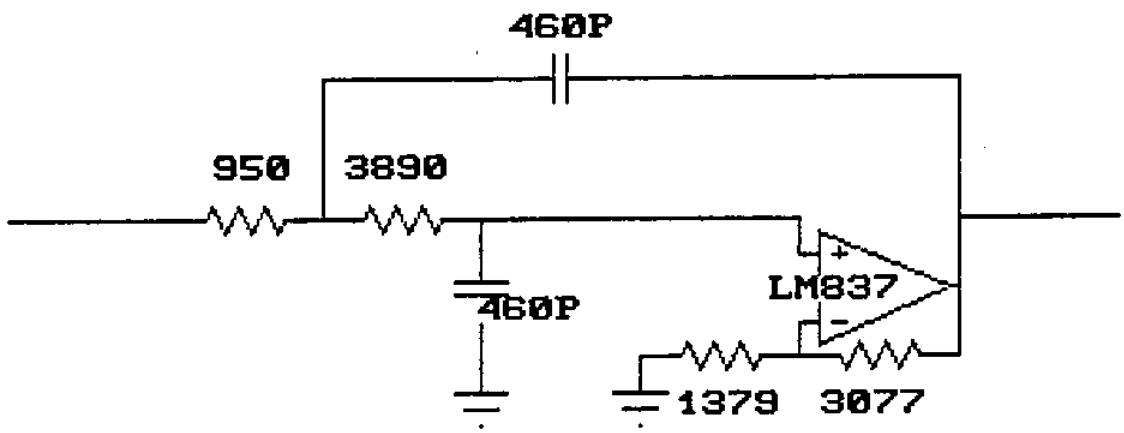

LOWPASS FILTER

FIGURE 15

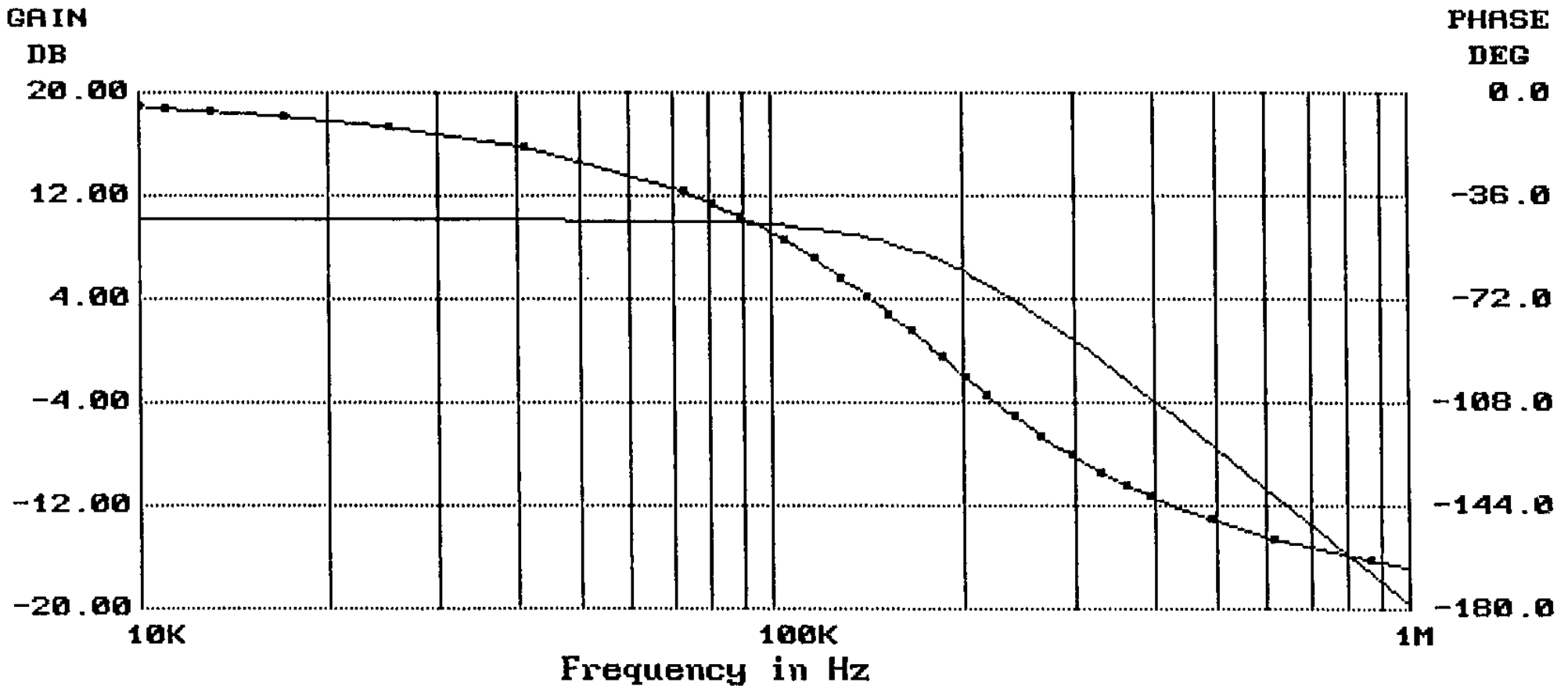

LOWPASS FILTER

FREQUENCY RESPONSE

FIGURE 16

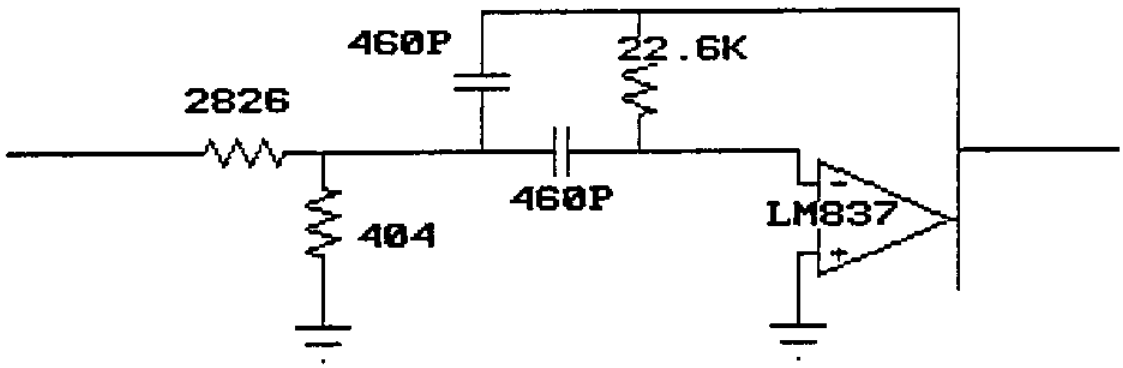

BANDPASS FILTER

FIGURE 17

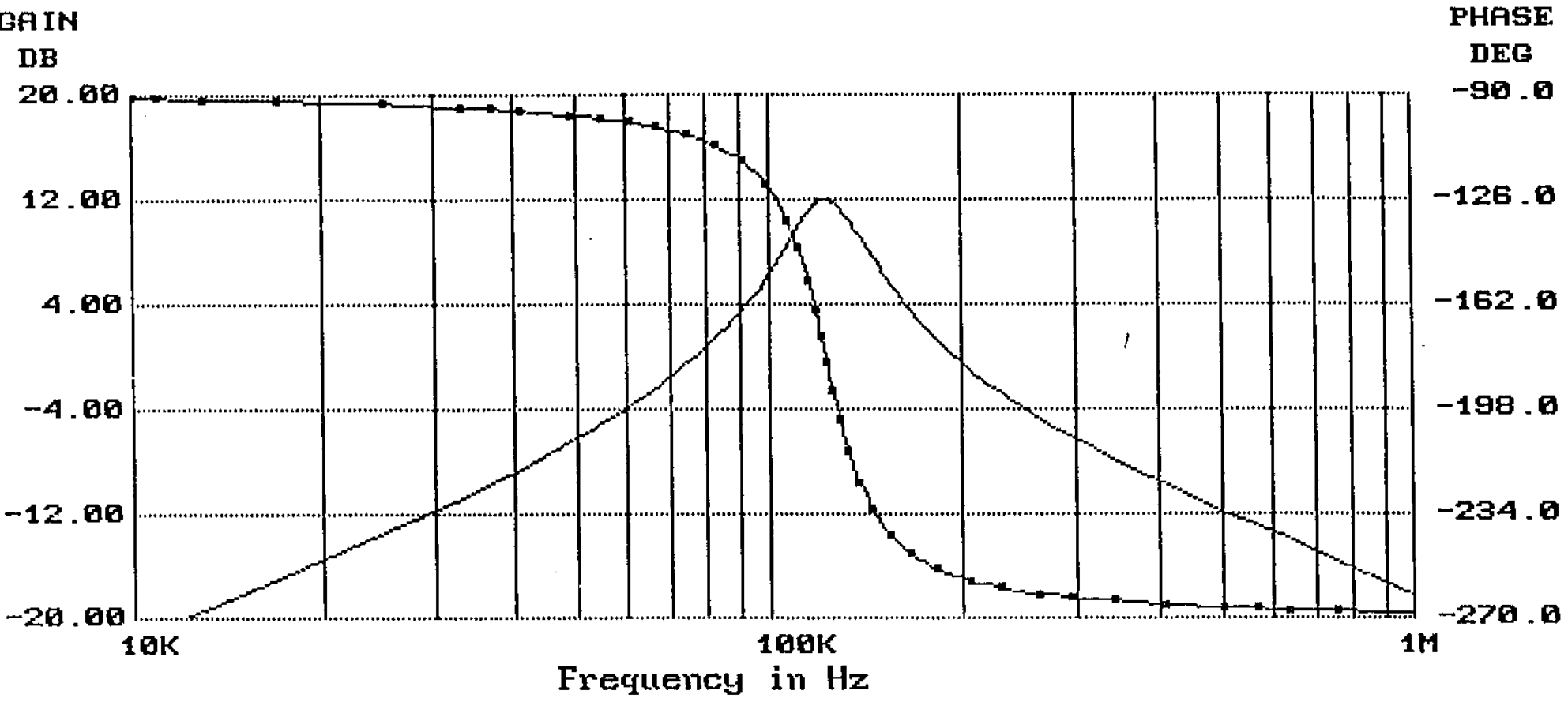

BANDPASS FILTER

FREQUENCY RESPONSE

FIGURE 18

filter. This was done so that any phase delay induced on the received signal by the first filter would also be induced on the reference signal. By doing this the phase difference between the two signals is due entirely to the propagation of the transmitted signal through the water.

While ideally the two filters will be the same, in practice there is likely to be some difference due to component tolerances. The ability to adjust the phase of filter two has therefore been incorporated into the design. The phase of the filter can be adjusted by adjusting the center frequency. This can be accomplished by adjusting the feedback resistor R_3. This will also change the gain of the filter. This however is not a concern in this specific application because equal gain is not essential.

6.3.3 - SIGNAL TRIGGERING

The signal, after being filtered, is converted into a square wave. This is accomplished using a high speed (300 V/μS) op-amp in an open loop configuration. The output was clamped between -.7 and +4.3 volts by a 4.3 volt zener diode to provide an appropriate input to the XOR gate. A 100Ω resistor was added to the output path of the op-amp as a current limiter.

6.3.4 - DIGITAL CIRCUITRY

The digital circuitry is designed to measure the magnitude of the phase difference between the reference and the transmitted signals. Using a 20 Mhz clock this phase difference is converted

to a time delay. The time delay is then stored in the computer for later use in determining the velocity of the transmitted signal. The digital circuitry is shown in figure 19. High speed CMOS chips were used for this purpose as they consume little power and exhibit fast switching times. The XOR gate acts as a phase difference detector. The output of the XOR gate is then ANDed with a 833.33μs pulse generated by the computer. The output of the AND gate is then ANDed with the 20 Mhz clock output. The output now consists of the number of 20 Mhz pulses that will fit within the phase difference of the two signals. This output is then used to increment the counter. The counter consists of two dual 4 bit counters cascaded to form a 16 bit counter. Once the counting is completed, the binary value in the counter is latched into the two 8 bit parallel in, serial out shift registers. This value is then shifted into the Tattletale using the built in SDI (Serial Data In) command of the computer. Once the data has been shifted into memory the software will cause the computer to set I/O pin 7 to a high value, clearing both counters and shift registers for the next value.

The CMOS circuitry, as well as the power applied to the 20 Mhz clock have been decoupled through the use of 0.1 uF capacitors placed between the power supply and ground.

7 - SOFTWARE

Software for this project has been written to store the incoming data from the sensors at the various measurement depths.

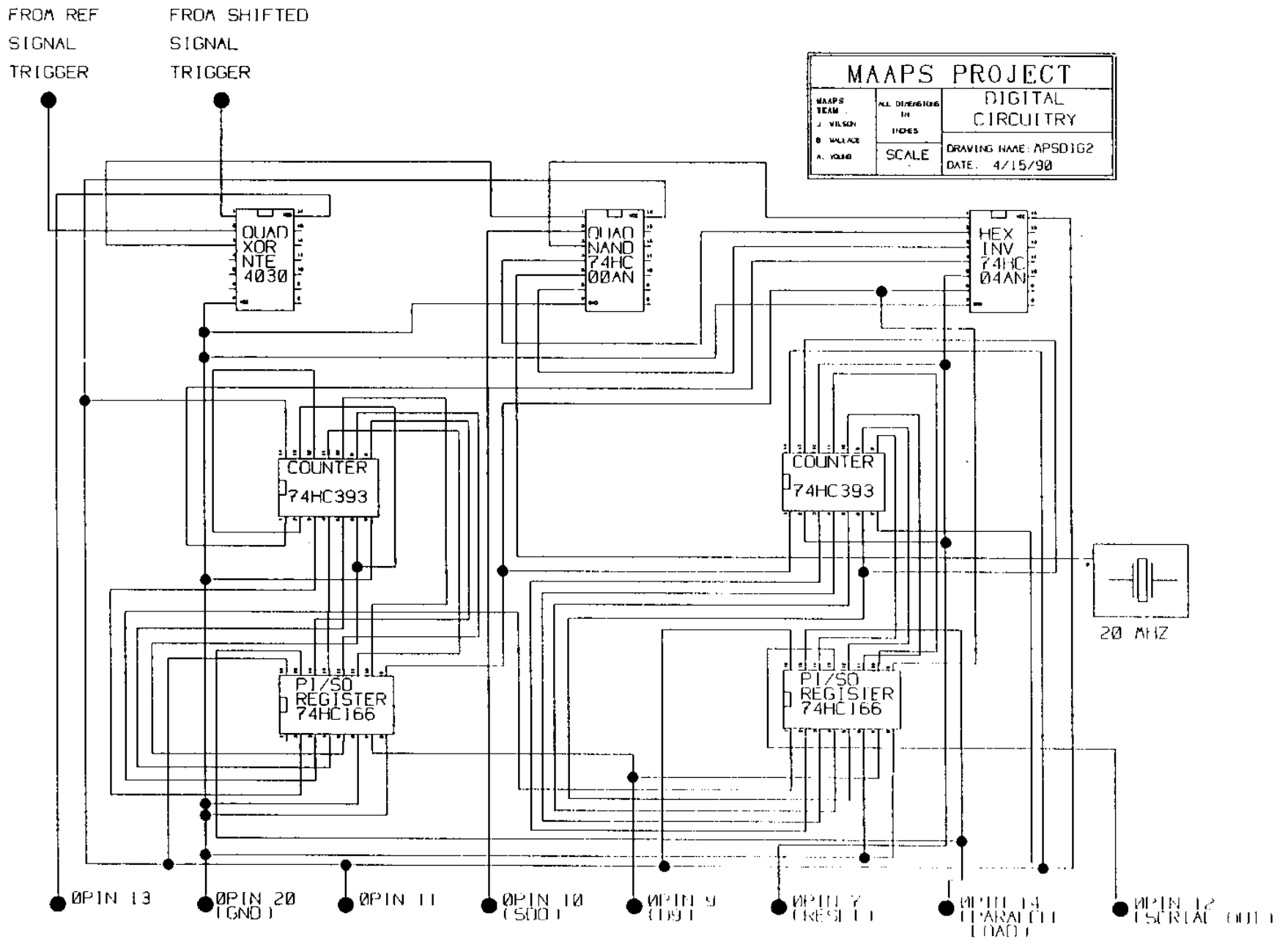
FROM REF SIGNAL TRIGGER
FROM SHIFTED SIGNAL TRIGGER
MAAPS PROJECT
MAAPS TEAM
J. WILSON
B. WALLACE
A. YOUNG
ALL DIMENSIONS IN INCHES
DIGITAL CIRCUITRY
SCALE
DRAWING NAME: APSDIG2
DATE: 4/15/90
QUAD XOR NTE 4030
QUAD NAND 74HC 00AN
HEX INV 74HC 04AN
COUNTER 74HC393
COUNTER 74HC393
20 MHZ
PI/SO REGISTER 74HC166
PI/SO REGISTER 74HC166
ØPIN 13
ØPIN 20 (GND)
ØPIN 11
ØPIN 10 (SDO)
ØPIN 9 (CLK)
ØPIN 7 (RESET)
ØPIN 14 (PARALLEL LOAD)
ØPIN 12 (SERIAL OUT)

FIGURE 19

Starting at the lowest possible memory location, the computer will store the following:

- thermistor value from A/D (1 byte)
- pressure transducer value from A/D (1 byte)
- phase delay pulse count from shift registers (2 bytes)

After filling the entire memory space (64K bytes), the computer will stop the data logging process. The data acquisition software takes advantage of the special functions built into the modified version of the BASIC language used by the TattleTale Model 3 computer. The data is offloaded from the instrument using the TATTLETOOLS FOR THE PC program from ONSET computers, manufacturers of the TattleTale. This program produces the output in a file suitable to be imported into MathCad for plotting purposes. The program listing can be found in appendix D.

8 - CONCLUSION

The complete mechanical structure for the project has been designed, built and tested at low depths. Included in the mechanical structure is the waterproof pressure vessel, the thermistor assembly, external computer interface, pressure transducer, and acoustic transducer assembly. Also designed and built was a sturdy cage to carry and protect the instrument.

Electronic hardware has been designed, built and tested to produce, filter, and condition the transmitted and received waveforms. The hardware consists of the analog wave shaping

circuitry, the digital pulse counting and computer interface circuitry, the regulated power circuitry, and the computer. All of these components have been successfully tested individually with the exception of the digital circuitry which awaits system integration.

As of this writing however, the instrument has not been tested as a complete system. The original conceptual design underwent several major modifications throughout the course of the year. Our original design was based on acoustic transmission between two piezoelectric transducers. To design the circuitry the frequency of the transducers was required. The operating frequency of the crystal with no mass loading is fairly easy to compute, based on its material properties. The frequency of the crystal however, is dramatically affected by any mass loading which may result from the physical mounting of the crystal to the mechanical structure. Research led to an estimate that the transducers would operate between 60 to 80 KHz based on previous mountings of similar transducer crystals. Based upon this frequency the circuitry for the system was designed. The actual mountings built for the transducers in this project however, resulted in enough variation in the operating frequency of the crystal to warrant redesigning the circuitry late in the project.

While testing of the instrument for actual data has been set back as a result of design changes, the major subsystems have proven operable for the desired application. In conclusion we are pleased with the fact that our design has proven so far to be a

feasible solution to the problem of directly measuring the velocity of sound underwater.

REFERENCES

1. Urick, Robert J. "Principles of Underwater Sound for Engineers" New York: McGraw-Hill, 1967.
2. Urick, Robert J. "Sound Propagation in the Sea" Los Altos: Peninsula Publishing, 1982.
3. McCalla, Jerrey M. "An Intelligent Systems Approach for the Improvement of High Frequency Acoustic Data Telemetry in Horizontally Isovelocity Shallow Water" Master of Science Thesis: U.N.H., 1989.
4. Kinsler, Frey, Coppens, & Sanders "Fundamentals of acoustics" New York: Wiley & Sons, 1982.
5. Smith, F.G. Walton "CRC Handbook of Marine Science, Vol. 1" Ohio: CRC Press, 1974.
6. Mechanical Properties Data Center, Belfour Stulen, Inc. "Aerospace Structural Metals Handbook, Vol. 3 Code 3206" Massachusetts: Department of Defense, 1975.
7. Myers, Holm, & McAllister "Handbook of Ocean and Underwater Engineering" New York: McGraw-Hill, 1969.
8. Juvinall "Stress, Strain, and Strength" New York: McGraw-Hill, 1967.
9. Shigley & Mischke "Mechanical Engineering Design" New York: McGraw-Hill, 1989.
10. Parker Seal Company "Parker O-Ring Handbook" Kentucky, 1974.
11. Franco "Design with Operational Amplifiers and Anolog Integrated Circuits" New York: McGraw-Hill, 1988.
12. Sedra & Smith "Microelectronic Circuits" New York: Holt, Rinehart & Winston, 1987.

APPENDIX A

Calculation of Pressure at 2500 ft.

Method 1: Pressure change per foot at 1000 m

= .447083 psi/ft. (p. 120, Ref. 5)

Pressure = (.447083 psi/ft)(2500ft) = 1118 psi

Method 2: $P = \rho g z$

$\rho \sim 1000$ Kg/m^3

$g = 9.8$ m/s^2

z = depth

$$z = \frac{(2500 \text{ ft})}{3.28 \text{ ft/m}} = 762 \text{ m}$$

$P = (1000 \text{Kg/m}^3)(9.8 \text{ m/s}^2)(762\text{m})$

P = 7.4676 x 10^6 Pa => 1083 psi

(1 lbf/in^2 = 6895 Pa)

*From these results a pressure of 1100 psi was used for calculation purposes.

Physical Data Table

Cylinder:

Outside Radius (r_o) = 4 in

Inside Radius (r_i) = 3.5 in

Wall Thickness (h) = .5 in

Pressure:

Outside Pressure (p_o) = 1100 psi

Inside Pressure = 0 psi

Material Properties:

(6061 T6 Aluminum, Drawn seemless tubing, .500 in. wall thickness)

Yield Strength (Fty) = 35 ksi (Table 3.015, Ref. 6)

Poissons Ratio (υ) = .33 (Fig. 3.061, Ref. 6)

Youngs Modulus (E) = 11,300 ksi (Fig. 3.062, Ref. 6)

Mode of Failure Analysis

A pressure vessel may fail by one of two means; exceeding the yield strength of the material, or by instability or buckling. The following calculations indicate which failure mode is the limiting case.

Calculation of Collapse Pressure (pressure to instability):

$$P_{cr} = \frac{E}{4(h-\upsilon^2)} \quad \frac{h^3}{R^3}$$

(eqn. 9-1, Ref. 7)

h = Wall thickness
R = Avg. radius
E = Modulus of elasticity
υ = Poissons ratio

$$P_{cr} = \frac{(11300 \times 10^3 \text{ psi})}{4(.5 \text{ in} - .33^2)} \quad \frac{(.5 \text{ in})^3}{(3.75 \text{ in})^3} = 17132.35 \text{ psi}$$

Calculation of Yielding Pressure (pressure to induce yielding):

$$P_y = \frac{(\sigma_y)(h)}{R_o}$$

(eqn. 9-3, Ref. 7)

σ_y = Yield strength
R_o = Outer radius

$$P_y = \frac{(35000 \text{ psi})(.5 \text{ in})}{4 \text{ in}} = 4375 \text{ psi}$$

*Since-- Py (4375 psi) < Pcr (17132.35 psi)
Failure will occur due to yielding.

Yielding Analysis for a Pressure Vessel

The total stress in a pressure vessel is a combination of three stresses.

Tangential Stress: $$\sigma_T = - \frac{(p_o)(r_o^2)}{r_o^2 - r_i^2} * \frac{(r^2 + r_i^2)}{r^2}$$ (eqn. 7.21 Ref. 8)

Radial Stress: $$\sigma_r = - \frac{(p_o)(r_o^2)}{r_o^2 - r_i^2} * \frac{(r^2 - r_i^2)}{r^2}$$ (eqn. 7.22 Ref. 8)

Axial Stress: $$\sigma_a = - \frac{(p_o)(r_o^2)}{r_o^2 - r_i^2}$$ (p. 114 Ref. 8)

p_o = outer pressure
r_o = outer radius
r_i = inner radius
$r = r_i$
(See Appendix A.2)

$$\sigma_T = - \frac{(1100 \text{ psi})(4 \text{ in})^2}{(4 \text{ in})^2 - (3.5 \text{ in})^2} * \frac{(3.5 \text{ in})^2 + (3.5 \text{ in})^2}{(3.5 \text{ in})^2} = -9387 \text{ psi}$$

$$\sigma_r = - \frac{(1100 \text{ psi})(4 \text{ in})^2}{(4 \text{ in})^2 - (3.5 \text{ in})^2} * \frac{(3.5 \text{ in})^2 - (3.5 \text{ in})^2}{(3.5 \text{ in})^2} = 0 \text{ psi}$$

$$\sigma_a = - \frac{(1100 \text{ psi})(4 \text{ in})^2}{(4 \text{ in})^2 - (3.5 \text{ in})^2} = -4693 \text{ psi}$$

Computation of a Factor of Safety

From Mohr's Circle for Stress (see Fig. A-1):

$$\sigma_1 = -9.387 \text{ ksi}$$
$$\sigma_2 = -4.693 \text{ ksi}$$
$$\sigma_3 = 0 \text{ ksi}$$
$$\tau_{max} = \frac{|-9.387 + 0|}{2} = 4.694 \text{ ksi}$$

S_y = Yield Strength

Maximum Normal Stress Failure Theory:

$$F.S. = \frac{S_y}{\sigma_1} = \frac{35 \text{ ksi}}{9.387 \text{ ksi}} = 3.73 \quad \text{(eqn. 6-2, Ref. 9)}$$

Maximum Shear Stress Failure Theory:

$$F.S. = \frac{S_y/2}{\tau_{max}} = \frac{35 \text{ ksi}/2}{4.694 \text{ ksi}} = 3.73 \quad \text{(eqn. 6-5, Ref. 9)}$$

Coulomb-Mohr. Failure Theory:

$$F.S. = \frac{S_y}{\sigma_1 - \sigma_3} = \frac{35 \text{ ksi}}{(9.387 - 0)\text{ksi}} = 4.22 \quad \text{(eqn. 6-14, Ref. 9)}$$

*The limiting case therefore gives a factor of safety of 3.73.

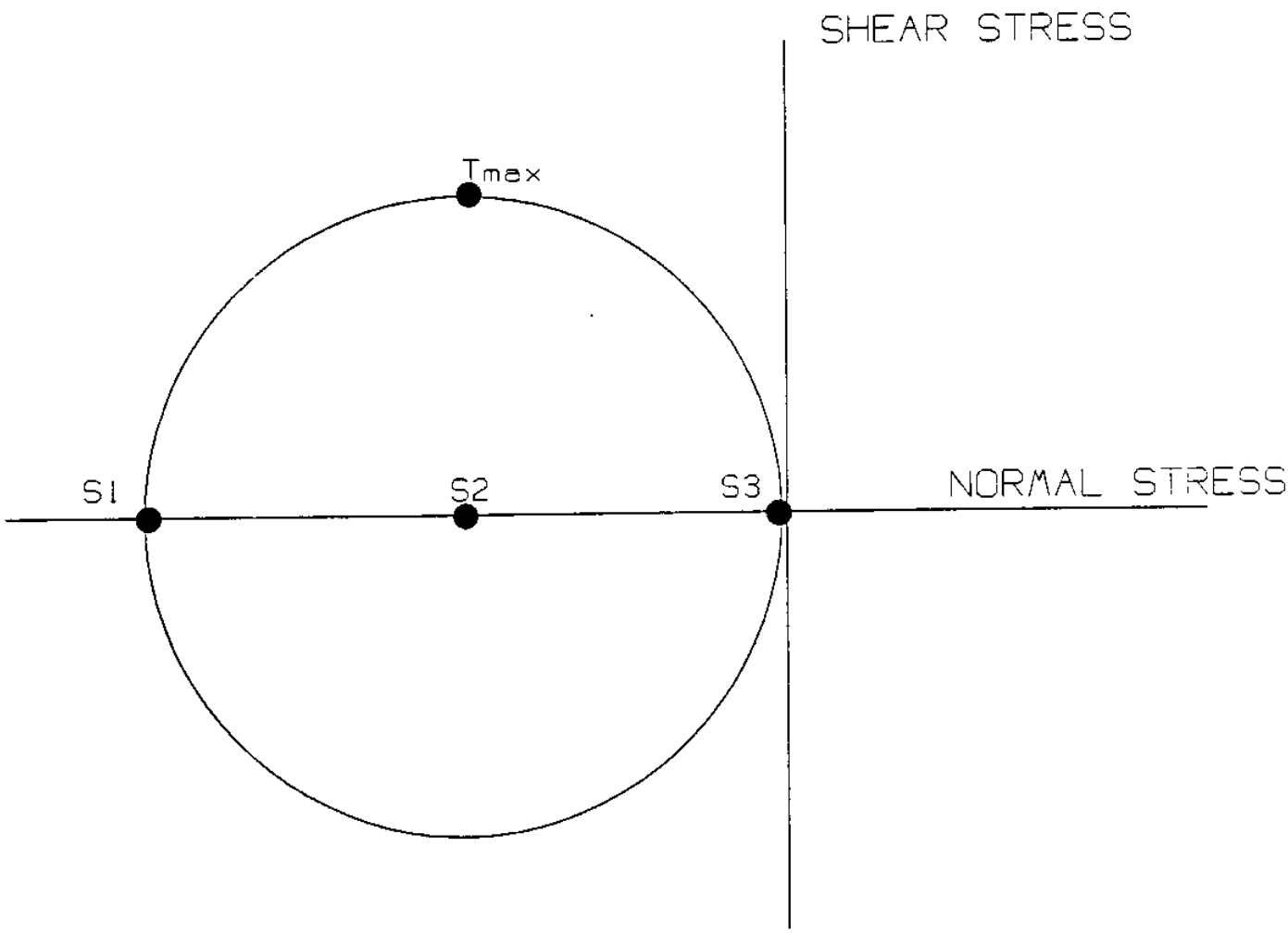

$S1 = \sigma_1 = -9.387$ ksi

$S2 = \sigma_2 = -4.693$ ksi

$S3 = \sigma_3 = 0$ ksi

$Tmax = \tau_{max} = \frac{\sigma_1 - \sigma_3}{2} = 4.694$ ksi

Mohr's Circle for Stress

Figure A-1

O-Ring Selection

Material Specification: The recommended compound number for sea water is: N674-70 (Table B5, Ref. 10)

- Nitrile Polymer
- Temp. Range -30/+250 °F

-It is recommended that Nitrile not be exposed to ozone, sunlight, or weather.

Size Specification: For the face seal between the end cap and the end of the cylinder the o-ring size number is:

2-264 (Table B6, Ref. 10)

- I.D. = 7.484 in. (+/- .030 in.)
- W = .139 in. (+/- .004 in.)

For the seal between the end cap and inside of the cylinder the o-ring size number is:

2-261 (Table B6, Ref. 10)

- I.D. = 6.734 in. (+/- .023 in.)
- W = .139 in. (+/- .004 in.)

APPENDIX B

Calculations of velocity,wavelenth and flight path

MAX VEL: 1540 m/s
MIN VEL: 1490 m/s

MAX VEL lambda = v/f = (1540 m/s)/120Khz = 12.833×10^{-3}m = 1.2833cm
MIN VEL lambda = v/f = (1490 m/s)/120Khz = 12.417×10^{-3}m = 1.2417cm

MAX - MIN = 416.67E-6 = 0.4167mm

MAX available space on endcap = 12.7 cm.

Based on needing 3 times the mass of transducer in back (housing) as in front of transducer, must have 1.09" Al. behind transducer, leaving 5", or 12.7 cm

Lambda average = 1.2625 cm

n(lambda/2) + (lambda/4) puts wave at antinode at RCVR transducer.

The maximum velocity is given by $v_{max} = (d_n/50n)f$ (1)
The minimum velocity is given by $v_{min} = (d_n/50(n+1))f$ (2)

For a safety factor of 2 $v_{max}-v_{min}$ should be at least 100m/s

For n=14
d_n = distance between transducers = 9.153 cm
v_{max} = 1569 m/s
v_{min} = 1465 m/s
$v_{max}-v_{min}$=104 m/s

Neither of these two velocities can reasonably be expected in water, so the velocities we are measuring will not shift out of the specified range.

Calculation for pulse width at output of XOR gate:
d_n = path length = 9.153 cm
$y = d_n$ - n(lambda)/2 = distance from node to transducer at time t=0 where the reference signal is just starting to go positive. (3)

PULSE WIDTH FOR LAMBDA = LAMBDA MAX (VEL = VEL MAX)

for lambda = lambda MAX = 1.283 cm (VEL = VEL MAX = 1540 m/s)
y = .172 cm
When node reaches xdcr, signal goes low. The time required for the

signal to go low (to cover the distance from the 8th node to the xdcr at a speed of 1540 m/s)is:

$$t_d = (y/v) \quad (4)$$
$$t_d = (.172\text{x}10^{-2}\text{m}/1540\text{m/s}) = 1.1175\mu\text{s}$$

After this time, the signal at the transducer goes low. (t_d=1.1175μs)
At t = 1.1175μs + T, signal goes high again.
t = 1.1175μs + 8.333μs = 9.4508μs

This results in an XOR gate output pulse width of

$$1/f - t_d \quad (5)$$

8.33μs - 1.1175μs = **7.2158μs** second pulse width.

See figure B.1

PULSE WIDTH FOR LAMBDA = LAMBDA MIN (VEL = VEL MIN)
Lambda min is solved similarly
Lambda min = 1.2417
y = .4612 cm

$$t_d = (.4612\text{x}10^{-2}\text{m})/1490 = 3.0953\mu\text{s sec}$$

At t = 3.095μs, transducer goes negative
At t = 11.423μs, transducer goes positive

This results in an XOR gate output pulse width of
8.333μs - 3.095μs = 5.2383μs

PW max - PW min = 1.9776μs

From equations (3), (4) and (5)

$$PW = 1/f_0 - (1/v)(d_n - nv/2f_0) \quad (6)$$

evaluated at f=120KHz
n=14
d_n=9.153x10^{-2}

$$\boxed{PW = 8.333\mu\text{s} - 1/v(9.153\text{x}10^{-2} - 58.33\text{x}10^{-6}v)}$$

From this equation the theoretical pulsewidths can be calculated from the velocities or the velocities from the measured pulsewidths.

If a minimum accuracy of 1 m/s is desired, 50 discreet velocities must be resolved. A range of 50 clock pulses should therefore be able to distinguish between the velocities.

This leads to the fraction 1.9776μs / 50 sections
= 39.55×10^{-9}s/section = 25 Mhz

The clock rate for sampling the the pulses cannot go much higher, so many periods of the wave must be added and averaged to allow to distinguish between the different velocities.

APPENDIX C

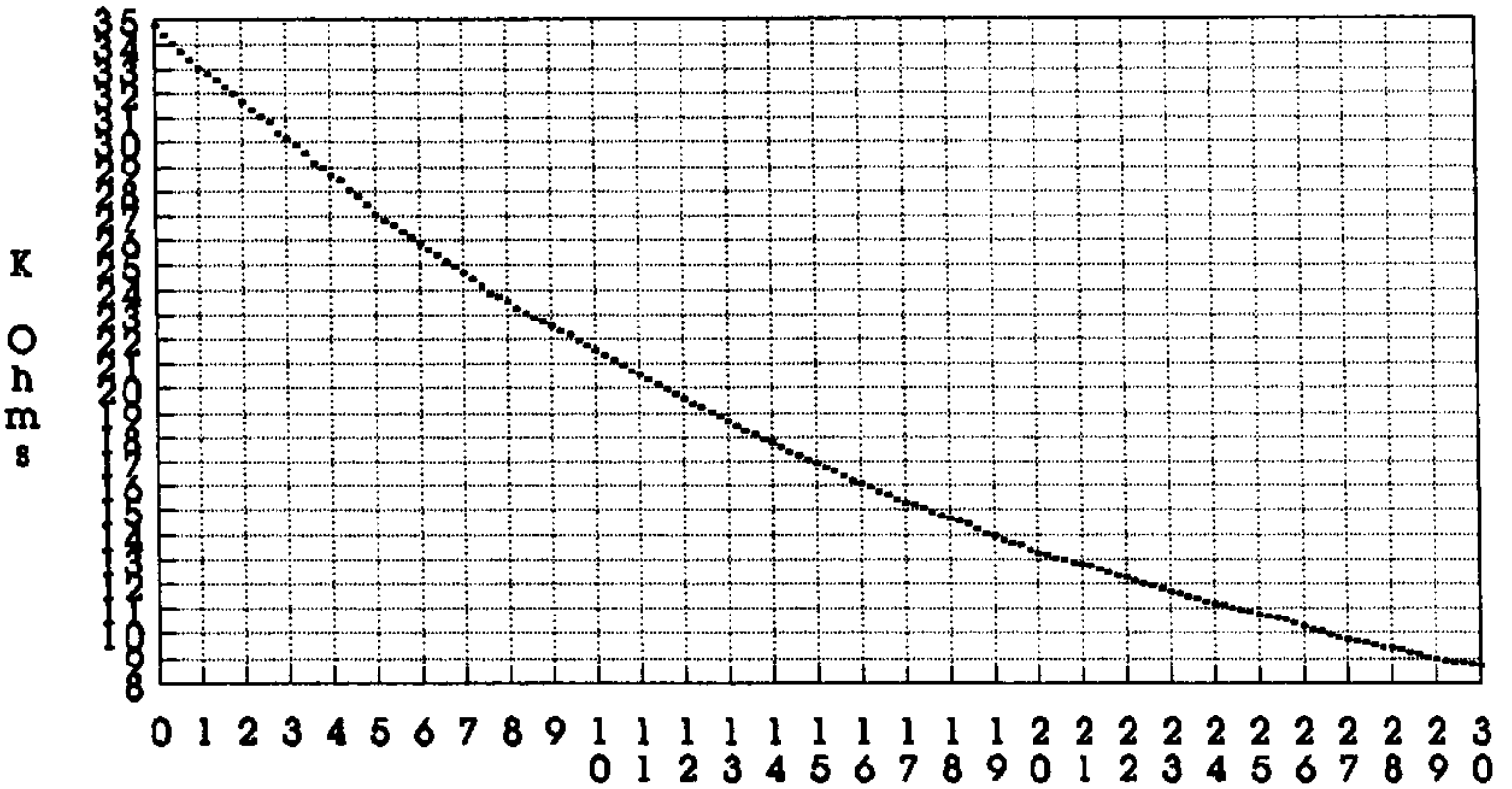

Appendix C.1
Resistance Characteristics

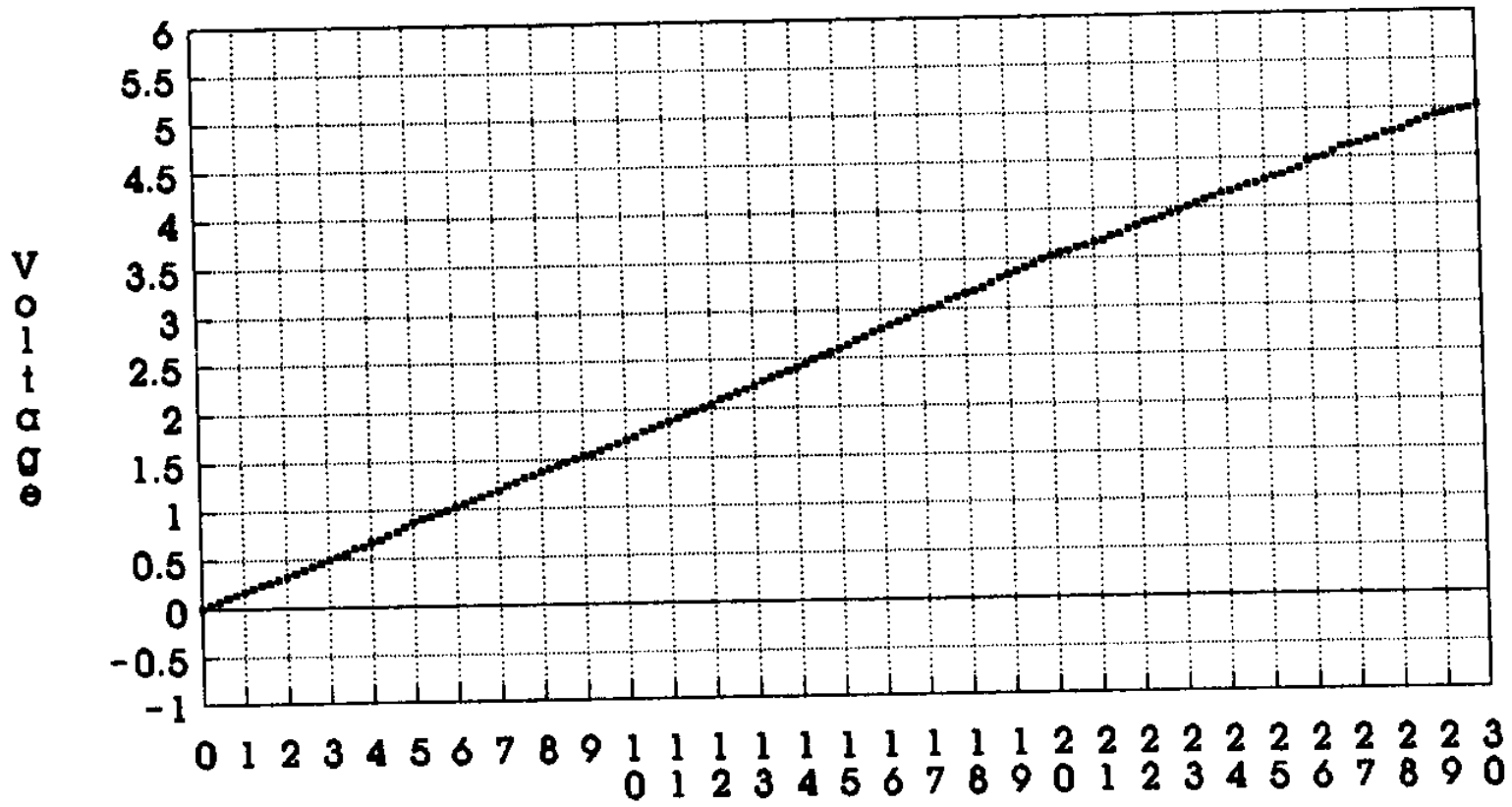

Appendix C.2
Wheatstone Bridge Output Voltages

Table of digital outputs corresponding to temperatures

Dig.	Analog	Temp	Digital	Analog	Temp
0	.019531	0	52	1.0352	6.0
1	.039063	0	53	1.0547	6.0
2	.058594	.2	54	1.0742	6.2
3	.078125	.4	55	1.0938	6.2
4	.097656	.4	56	1.1133	6.4
5	.11719	.6	57	1.1328	6.6
6	.13672	.6	58	1.1523	6.6
7	.15625	.8	59	1.1719	6.8
8	.17578	.8	60	1.1914	6.8
9	.19531	1.0	61	1.2109	7.0
10	.21484	1.2	62	1.2305	7.0
11	.23438	1.4	63	1.25	7.2
12	.25391	1.4	64	1.2695	7.2
13	.27344	1.6	65	1.2891	7.4
14	.29297	1.8	66	1.3086	7.4
15	.3125	1.8	67	1.3281	7.6
16	.33203	2.0	68	1.3477	7.6
17	.35156	2.0	69	1.3672	7.8
18	.37109	2.2	70	1.3867	8.0
19	.39063	2.4	71	1.4063	8.0
20	.41016	2.4	72	1.4258	8.2
21	.42969	2.6	73	1.4453	8.2
22	.44922	2.6	74	1.4648	8.4
23	.46875	2.8	75	1.4844	8.6
24	.48828	2.8	76	1.5039	8.6
25	.50781	3.0	77	1.5234	8.8
26	.52734	3.2	78	1.5430	9.0
27	.54688	3.2	79	1.5625	9.0
28	.56641	3.4	80	1.5820	9.2
29	.58594	3.4	81	1.6016	9.4
30	.60547	3.4	82	1.6211	9.4
31	.62500	3.6	83	1.6406	9.6
32	.64453	3.8	84	1.6602	9.6
33	.66406	3.8	85	1.6797	9.8
34	.68359	4.0	86	1.6992	9.8
35	.70313	4.2	87	1.7188	10.0
36	.72266	4.2	88	1.7383	10.2
37	.74219	4.4	89	1.7578	10.2
38	.76172	4.4	90	1.7773	10.4
39	.78125	4.6	91	1.7969	10.4
40	.80078	4.6	92	1.8164	10.6
41	.82031	4.8	93	1.8359	10.6
42	.83984	4.8	94	1.8555	10.8
43	.85938	4.8	95	1.875	10.8
44	.87891	5.0	96	1.894	11.0
45	.89844	5.0	97	1.914	11.0
46	.91797	5.2	98	1.933	11.2
47	.93750	5.4	99	1.953	11.2
48	.95703	5.4	100	1.972	11.4
49	.97656	5.6	101	1.992	11.6
50	.99609	5.8	102	2.011	11.6
51	1.0156	5.8	103	2.031	11.8

Dig.	Analog	Temp.	Dig.	Analog	Temp
104	2.0508	11.8	157	.0859	17.6
105	2.0703	12.0	158	.1055	17.6
106	2.0898	12.0	159	.1250	17.8
107	2.1094	12.2	160	.1445	17.8
108	2.1289	12.2	161	.1641	18.0
109	2.1484	12.4	162	.1836	18.2
110	2.1680	12.6	163	.2031	18.2
111	2.1875	12.6	164	.2227	18.4
112	2.2070	12.8	165	.2422	18.4
113	2.2266	12.8	166	.2617	18.6
114	2.2461	13.0	167	.2813	18.6
115	2.2656	13.0	168	.3008	18.8
116	2.2852	13.2	169	.3203	18.8
117	2.3047	13.2	170	.3398	19.0
118	2.3242	13.4	171	.3594	19.0
119	2.3438	13.4	172	.3789	19.2
120	2.3633	13.6	173	.3984	19.2
121	2.3828	13.6	174	.4180	19.4
122	2.4023	13.8	175	.4375	19.4
123	2.4219	13.8	176	.4570	19.6
124	2.4414	14.0	177	.4766	19.6
125	2.4609	14.2	178	.4961	19.8
126	2.4805	14.2	179	.5156	19.8
127	2.5000	14.4	180	.5352	20.0
128	2.5195	14.4	181	.5547	20.2
129	2.5391	14.6	182	.5742	20.2
130	2.5586	14.6	183	.5938	20.4
131	2.5781	14.8	184	.6133	20.6
132	2.5977	14.8	185	.6328	20.8
133	2.6172	15.0	186	.6523	20.8
134	2.6367	15.0	187	.6719	21.0
135	2.6563	15.2	188	.6914	21.2
136	2.6758	15.2	189	.7109	21.2
137	2.6953	15.4	190	.7305	21.4
138	2.7148	15.4	191	.7500	21.6
139	2.7344	15.6	192	.7695	21.6
140	2.7539	15.6	193	.7891	21.8
141	2.7734	15.8	194	.8086	21.8
142	2.7930	15.8	195	.8281	22.0
143	2.8125	16.0	196	.8477	22.0
144	2.8320	16.2	197	.8672	22.2
145	2.8516	16.2	198	.8867	22.4
146	2.8711	16.2	199	.9063	22.4
147	2.8906	16.4	200	.9258	22.6
148	2.9102	16.6	201	.9453	22.6
149	2.9297	16.6	202	.9648	22.8
150	2.9492	16.6	203	.9844	23.0
151	2.9688	16.8	204	.0039	23.0
152	2.9883	17.0	205	.0234	23.2
153	3.0078	17.0	206	.0430	23.2
154	3.0273	17.2	207	.0625	23.4
155	3.0469	17.4	208	.0820	23.6
156	3.0664	17.4	209	.1016	23.6

Dig.	Analog	Temp
210	4.1211	23.8
211	4.1406	23.8
212	4.1602	24.0
213	4.1797	24.2
214	4.1992	24.4
215	4.2188	24.4
216	4.2383	24.6
217	4.2578	24.8
218	4.2773	24.8
219	4.2969	25.0
220	4.3164	25.2
221	4.3359	25.4
222	4.3555	25.4
223	4.3750	25.6
224	4.3945	25.6
225	4.4141	25.8
226	4.4336	25.8
227	4.4531	25.8
228	4.4727	26.0
229	4.4922	26.2
230	4.5117	26.2
231	4.5313	26.4
232	4.5508	26.4
233	4.5703	26.6
234	4.5898	26.6
235	4.6094	26.8
236	4.6289	26.8
237	4.6484	27.0
238	4.6680	27.2
239	4.6875	27.4
240	4.7070	27.6
241	4.7266	27.6
242	4.7461	27.8
243	4.7656	28.0
244	4.7852	28.2
245	4.8047	28.2
246	4.8242	28.2
247	4.8438	28.4
248	4.8633	28.6
249	4.8828	28.6
250	4.9023	28.8
251	4.9219	28.8
252	4.9414	29.0
253	4.9609	29.2
254	4.9805	29.4
255	5.0000	29.6

APPENDIX D

DATA ACQUISITION SOFTWARE LISTING

```
100 REM    DATA ACQUISITION PROGRAM FOR THE TATTLETALE MODEL 3
110 REM    WRITTEN BY ALAN W. YOUNG 4/15/90
120        X=0 : REM SET MEMORY POINTER TO 0
130        PSET 0 : REM RESETS COUNTERS AND PI/SO SHIFT REGISTERS
140        PSET 3 : REM LATCH INHIBITED UNTIL DATA SHIFTED IN
150        SLEEP 0 : REM SYNC SLEEP FUNCTION
160        ONERR 300 : REM WHEN MEMORY IS FULL JUMP TO END
170        SLEEP 100 : REM WAIT .1 SECONDS TILL NEXT CONVERSION
180        REM BURST CONVERT FIRST TWO A/D CHANNELS (THERMISTOR AND
190        REM PRESSURE TRANSDUCER) AND STORE IN MEMORY
200        BURST X,2
210        REM PRODUCE ONE CYCLE OF SQUARE WAVE OF PERIOD ****
220        REM WHICH WILL TRIGGER START OF COUNTER CLOCKING
230        TONE 230,1
240        REM LATCH PHASE SHIFT DELAY INTO PI/SO REGISTERS, AND
250        REM SHIFT IN 16 BITS OF DATA, MSB FIRST USING SDI
260        REM SERIAL DATA IN COMMAND
270        LET A=SDI 16
280        STORE A
290        GOTO 130 : REM REPEAT CALCULATION
300        REM MEMORY FULL
310        STOP
```